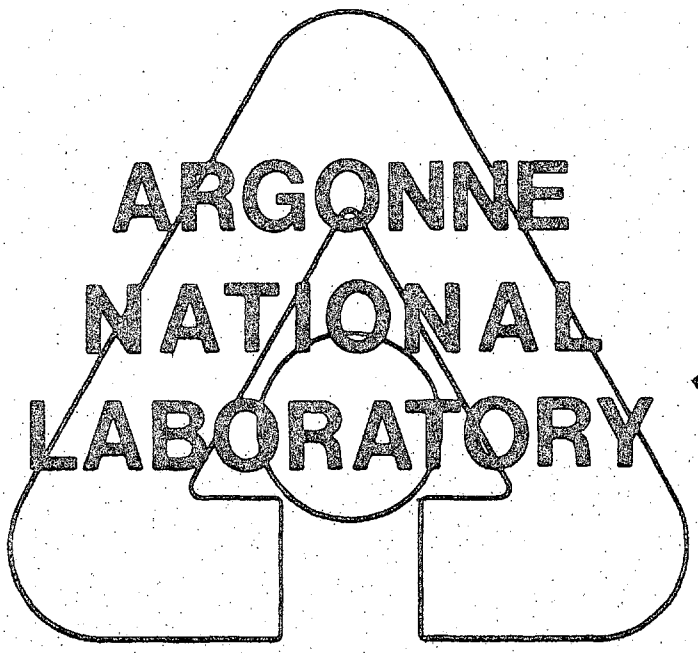

U of C-AUA-USAEC

Relative and Absolute Measurements of the Fast Neutron Fission Cross Section of ^{235}U

W. P. Poenitz

Argonne National Laboratory

Relative and Absolute Measurements of the Fast Neutron Fission Cross Section of ^{235}U*

W. P. Poenitz

Argonne National Laboratory

*Work performed under the auspices of the U S Atomic Energy Commission.

ABSTRACT

Measurements of the shape of the ^{235}U fission cross section were carried out in the energy range from 35 keV to 3.5 MeV. Three different techniques were applied to monitor the neutron flux. The $^{6}Li(n,\alpha)T$ cross section was utilized in the lower energy range (< 110 keV). The Grey Neutron Detector was employed in the entire energy range, and the Black Neutron Detector was used above 400 keV. The shape values were normalized with the results obtained from three different sets of absolute cross section measurements. The associated activity technique was applied in the 450-650 keV range, the Black Neutron Detector was used for absolute flux measurements at 800 keV and 3.5 MeV, and a calibrated vanadium-bath was used at 500 keV.

The results from the present measurements agree well with more recent data obtained by other experimenters but differ up to a factor of two from older values.

INTRODUCTION

The fission cross section of ^{235}U has a unique importance for the evaluation and design of fast breeder reactors for which ^{235}U is a major reference cross section. The importance of the absolute ^{235}U fission cross section is furthermore emphasized by its use as a reference cross section in most other fission cross section measurements as well as some capture and reaction cross section measurements, and as a flux monitor. Data existing at the beginning of the present measurements (1971) differed by more than a factor of two (Ref. 1-28). A general downward trend of the cross section data was observed when the experimental results were correlated as a function of the time of their measurement (29). More recent data show differences in the 6-15 per cent range. However, some newer absolute ^{235}U fission cross section measurements are contradicted by values obtained from other absolute cross sections ($^{6}Li(n,\alpha)^{7}Be$, $^{197}Au\ (n,\gamma)\ ^{198}Au$, and $^{238}U(n,\gamma)^{239}U$) and appropriate ratio measurements (23, 29, 65), which suggest 5-15 per cent lower ^{235}U fission cross sections. Lower ^{235}U fission cross sections were supported by measurements by Gorlove et al. (18) and some preliminary data (23) which were obtained with the same experimental technique as applied to measurements of the absolute capture cross sections. The latter had revealed the discrepancy in the ^{235}U cross section. Because of the importance of the ^{235}U fission cross section and its uncertainty, a program was initiated to measure this cross section over a large energy range.

Measurements in the low keV-energy range are usually carried out relative to the well known cross section shapes of $^{6}Li(n,\alpha)T$ or $^{10}B(n,\alpha)^{7}Li$. In the higher MeV-energy range measurements relative to the hydrogen scattering cross section should result in reliable data. The "gap" from $\sim$ 50 keV to $\sim$ 2 MeV is

of major interest for real power reactors but is difficult for absolute neutron flux measurements (30-33), and a wide variety of techniques have been employed in the past. Many of these measurements resulted in discrepant values. Thus, the present measurements were designed to use several independent techniques with overlapping energy ranges so that the results bridged the gap from the low keV range to the higher MeV range. The objective was results not only independent of the flux determination, but also of experimental techniques and fissile samples. The uncertainty objective of the present measurements ($\sim$ 3%) was chosen to resolve the existing discrepancies of the ^{235}U cross section.

NEUTRON SOURCES

The $^{7}Li(p,n)^{7}Be$- and the $^{51}V(p,n)^{51}Cr$-reactions were used as neutron sources. The majority of the measurements were carried out with the accelerator in a pulsed mode and the time-of-flight technique was used for background suppression. The primary proton beam was pulsed and bunched to about 1-2 nsec. width and accelerated by a Van de Graaff or a Tandem-Dynamitron. The repetition rate was 1 or 2 MHz. All data were taken with thin targets, yielding essentially "monoenergetic" neutrons.

The $^{7}Li(p,n)^{7}Be$-reaction was used in most of the measurements. This neutron source has a high yield, is simple to use, and requires no safety precautions. The reaction and its features as a neutron source are well documented (see for example Ref. 34). For the present experiments targets were made from metallic lithium evaporated on a 0.025 cm thick tantalum backing. The target backing is a cylindrical cup with a diameter of 7 cm and a height of 4 cm. The relative yield of the second neutron group existing above $\tilde{\sim}$ 2.4 MeV primary energy is well known (35, 36) and requires only a small correction in most of

the present experiments. The energy range of the present measurements did not exceed the threshold for the $^{7}Li(p,^{3}He,n)^{4}He$-reaction, and contributions from the Ta(p,n)-reaction in the target backing were small (36). The average neutron energy was determined from the primary energy, the target thickness, and the stopping cross sections using the well known kinematic relations. The uncertainties of the energy determination were estimated to be ± 3 keV.

The $^{51}V(p,n)^{51}Cr$-reaction was used to obtain "monoenergetic" neutrons in the energy range from 450-600 keV. This reaction is a favorable neutron source for use with the associated activity technique. Vanadium was evaporated on a backing (silver, 0.05 cm thick, or tantalum, 0.035 cm thick) with thicknesses in the range 0.5 - 1.2 mg/cm^2. A layer of 0.2 - 0.4 mg/cm^2 silver was evaporated on top of the vanadium. This silver layer prevented the loss of ^{51}Cr-activity due to thermal evaporation. The average energy was evaluated from the known primary energy and the thicknesses of the silver and vanadium layers. The angular distribution of the $^{51}V(p,n)^{51}Cr$-reaction is known to be fairly isotropic in the range of the present measurements (37), however, an additional measurement was carried out at 600 keV. Two Long Counters were used for this measurement. One was positioned at 90° as a monitor, and the other was used for the measurements at different angles. No correction was applied for the change of the counter efficiency as it should have been nearly constant in the 100 keV energy interval of the measurement. The anisotropy was found not to exceed 15 per cent.

FISSION DETECTORS AND FISSILE SAMPLES

Many types of fission detectors were described in the past (38). In the present experiment both gas scintillation counters and ionization chambers were used. For the gas scintillation counters a mixture of 85 per cent argon and 15 per cent nitrogen was employed as scintillation gas and passed continuously

through the chamber so as to remove poisons. Methane was used for the ionization chamber, in a similar continuous-flow mode.

2π-Gas Scintillation Counter (2π-GSC)

The gas chamber of the counter was designed to reduce the scattering background from the chamber walls, photomultipliers and other structural materials (see Fig. 1). The chamber had a cylindrical shape with a diameter of 22 cm and a height of 16 cm. The thickness of the iron-wall was 0.03 cm. Thin aluminum foil was used as a light reflector at the walls. The fissile sample was placed axially at one end of the gas scintillation counter. The molybdenum backing of the sample constituted the counter wall at this position. The scintillation light produced by the fission fragments in the gas scintillator was viewed by four RCA 7850 photomultipliers placed at the side of the scintillation chamber. The fast anode output signals were added in pairs and the coincidence technique was applied to exclude signals caused by fast neutrons in the multipliers. The time-resolution of the counter was about 3 nsec. A fission fragment energy spectrum obtained with this counter is shown in Fig. 1.

4π-Gas Scintillation Counter (4π-GSC)

A double-chamber gas-scintillation counter described previously (39) was used as a counter in conjunction with a fissile deposit on a thin backing which permitted the transmission of fission fragments. The fission foil was placed in the center of the counter, between the two chambers (see Fig. 2). The signals obtained from both chambers were added, thus a summation of the light produced by both fission fragments was obtained. This improved the fission fragment energy spectra measurement by reducing the necessary extrapolation to zero pulse height. A fission fragment pulse height spectrum obtained with this counter is shown in Fig. 2.

The Spherical Fission Counter (SS-IC)

A spherical fission counter was designed to utilize the 4π-neutron yield from the $^{51}V(p,n)^{51}Cr$-reaction. The counter, shown in Fig. 3, consisted of two spherical shells of 3.8 cm and 6.4 cm radii. The shells were made of silver sheets 0.025 to 0.05 cm thick. They are separated and held in position by three teflon rods of 0.4 cm diameter and 2.5 cm length and a teflon ring which forms an entrance channel (0.025 cm thick) for the proton beam tube (0.03 cm thick, 0.95 cm diameter). The counter was operated as an ionization chamber using methane as a gas flowing continuously through the counter.

The uranium was deposited by molecular plating on the polished outside surface of the inner sphere. The α-count rate was measured with the spherical counter itself using appropriate amplification of the output pulses. Three spheres were used in the experiments plated with uranium of two different isotopic compositions. The surface area of each sphere was determined from a sampling of the diameter and from volume measurements.

The spacial distribution of the uranium deposit on the spheres was determined with a surface-barrier detector by measuring the α-particles at different positions on the sphere. The deposits were found to be uniformly distributed within $\pm$ 5 per cent. A fission fragment energy spectrum obtained with this counter is shown in Fig. 3. No timing was used with the spherical ionization chambers.

Fast-Timing Ionization Chamber (FT-IC)

An ionization chamber designed for fast timing by Meadows (40) was used in some measurements (see Fig. 4). The collector plate was made of 0.013 cm thick, 7.0 cm diameter, molybdenum, and positioned at 0.6 cm distance from the fission foil which, in turn, was 1.2 cm away from the counter wall. A pulse height

spectrum obtained with this counter is shown in Fig. 4. The time resolution of this counter was about 4 nsec.

Fissile Samples and Mass Assignments

Features of the fissile samples used in the present experiments are summarized in Table I. Accurate determinations of the surface area was required for only some of the samples. For the spherical samples, area-measurements were obtained from a sampling of the diameter, and from volume-determinations. The use of the foils in the different counters is indicated in the table. The different fissile materials used on the foils are described in Table II. The isotopic compositions are given in this table. Results were available from several analysers. Those given in the table were used for correcting fission events in isotopes other than ^{235}U. Mass assignments for samples used in absolute measurements were required and the values are also given in Table II. The values were obtained from α-counting the samples and the specific activity of the material used. The α-counting was carried out in low geometry for the disc-shaped samples and in the counter itself for the spherical samples. The uncertainty for the low geometry α-counting was $\leq$ 0.2 per cent and 1.5 per cent for the counting in the spherical counters. The latter required a correction of 0.6 per cent for the total absorption of α-particles and 1.2 per cent for α-recoils.

The specific activities were determined by three different techniques using different samples of the same material:

a) The isotopic composition was obtained from mass spectroscopic analysis. The half-lives $T_{1/2}(^{234}U) = (2.443 \pm 0.011)\ 10^5$ Y (41,42,33), and $T_{1/2}(^{235}U) = (7.02 \pm 0.08)\ 10^8$ Y (43), and those for other isotopes as quoted in nuclide charts, were used to derive the specific activities.

b) Samples were α-counted in low-geometry or 2π-geometry and the mass was obtained from an analysis by mass spectroscopic isotopic dilution technique.

c) Samples were α-counted in low-geometry or 2π-geometry and the mass was obtained by colorimetric mass analysis.

Several values were obtained with each technique for the material U-3 which is the most important for the present measurements. The results for the specific mass is shown in Fig. 5. The good agreement between the averages from the different techniques is deceptive because of the scattering of the single points. However, an uncertainty of ∿ 0.5 per cent was estimated from the agreement between the results from the isotopic dilution technique and those based on the isotopic spectroscopy and the half-lives.

The specific activity of the material U-4 is based on the colorimetric analysis of ∿ 30 samples (44), four different analyses by mass spectroscopy, and the above cited half-lives.

The masses of the fissile materials on the spherical counters were originally determined from the destructive colorimetric analysis of these spheres (26). However, subsequent determinations of the specific activity of the material by the mass spectroscopic isotopic dilution technique casts some doubt on these results and the values given in Table II are based on the α-count rate obtained with the spheres and an additional series of determinations of the specific activities of the materials involved by the above quoted techniques.

Detection Efficiency of Fission Counters

The major factors which govern the detection efficiency for fission events in the sample are the total absorption of both fission fragments in the sample and the loss of pulses due to an electronic or digital (-computer) threshold.

A linear dependence of the total fission fragment absorption was reported by White (20). In contrast to these results much higher values were quoted by Knobeloch (45) and Deruytter (46). This situation was discussed extensively by Deruytter (46), however, recent measurements by Meadows (47) support a linear dependence of the total fission fragment absorption down to 50 $\mu g/cm^2$ thickness of the fissile material. Thus, in the present experiments, corrections obtained from the interpolation between White's and Meadows' results were used.

The total absorption of fission fragments in the 4π-foil was obtained by evaluating the total absorption for both, 2π- and 4π- foils with the Monte Carlo technique. An average path length of the fission fragments was assumed and adjusted so that the total absorption as measured for a 2π-foil by White (20) and Meadows (47) was reproduced. Then the evaluated result for the 4π- foil was used to correct the total fission fragment absorption.

The number of pulses lost below the threshold setting for counting fission fragments was determined by extrapolating to zero pulse height as indicated in the Figs. 2, 3 and 4.

Some smaller but energy-dependent corrections for the fission detector efficiency were applied. The momentum of the incoming neutron changes the total fission fragment absorption, and the angular distribution of the fission fragments is a function of the primary neutron energy (38). Even though the energy dependence of the latter effect is negligible for ^{235}U, the former requires a correction of up to 0.5 per cent for the thicker foils in the present energy range of up to 3.5 MeV. Corrections for fission events in isotopes other than ^{235}U were usually small (< 0.1 per cent) due to the purity of the fissile materials. For the fissile material U-4, the correction at 800 keV was 0.9 per cent and for U-5 up to 1.2 per cent.

NEUTRON DETECTORS

A large variety of neutron detectors were designed and described in the past (48). The detectors used in the present experiments were selected and specially designed to suit these particular cross section measurements.

The Black Neutron Detector (BND)

The fast neutron flux is often determined with proton recoil counters (49) utilizing the well-known total cross section of hydrogen. The flux measurements with these detectors depends on the knowledge of the scattering cross section of hydrogen and its angular distribution, the active volume of the counter, the amount of hydrogenous material, the extrapolation to zero pulse height etc., depending on the type of the detector which is used. For the present measurements a total energy conversion detector was designed for the measurement of the absolute neutron flux which was based on the detection of proton recoils but did not depend in first order on the above cited effects and cross sections. The detector is a medium sized scintillator of cylindrical shape with a neutron entrance channel terminated at about the center of the cylinder. The neutrons enter through the channel and lose most of their kinetic energy in successive collisions with the hydrogen and carbon nuclei in the scintillator. The scintillation light produced by the recoil nuclei is detected with several photomultipliers. The detector allows the application of the time-of-flight technique and results in a favorable recoil-energy sum-spectra; requiring only a small correction for the extrapolation to zero pulse-height. This detector and a detailed Monte Carlo evaluation of the second order effects are described elsewhere (50-52). Two different BND detectors were used in the present experiment. The smaller detector was a plastic scintillator with aradius of 8.8 cm and a length of 30 cm. The central entrance channel was 15.2 cm long and had a

diameter of 2.5 cm. Five 58 AVP photomultipliers were used to detect the scintillation light. The larger detector was a liquid scintillator in a cylindrical container with a radius of 13 cm, a length of 35.5 cm, and an entrance channel with a diameter of 2.5 cm and a length of 11.5 cm. Four 58 AVP photomultipliers were used with this detector. The efficiency of the smaller detector is shown in Fig. 6. The larger detector was used at 3.5 MeV only and its efficiency was 96.7 per cent at that energy. The time-of-flight spectrum and the energy pulse height spectrum obtained with the larger detector at 3.5 MeV are shown in Fig. 7.

The Grey Neutron Detector (GND)

The Grey Neutron Detector (51-54) was used as a relative neutron flux monitor in the cross section shape measurements and after calibration with Cf-252 sources, for an absolute measurement at 500 keV. The detector consists of a moderator volume with an entrance channel for the primary neutron beam. The neutrons are slowed down and captured in the moderator. The prompt capture γ-rays are detected at the surface of the moderator with a NaI(Tl)-detector. The efficiency is a smooth and flat function of the primary energy. This detector was described in detail on various occasions (53-55, 51). For the present measurements, two different detector sizes and four different moderator materials were used in order to check for a possible influence of the non-constant efficiency on the measured results. The smaller detector was a paraffin cube with a side length of 60 cm. The larger detector was a container filled with about 400 liters of pure water, a $MnSO_4$ solution or a $VOSO_4$ solution. For the paraffin and the water moderators the 2.2-MeV capture γ-ray from hydrogen was utilized. For the $MnSO_4$ solution the high energy capture γ-rays of manganese were detected. For the $VOSO_4$ solution the high energetic γ-rays from the capture

in vanadium and the 2.2-MeV capture γ-ray from hydrogen were used. The two different efficiencies for the latter are shown in Fig. 8 as a function of energy. The ratios of the relative neutron fluxes measured with the two different portions of the γ-spectra, as indicated in Fig. 8, do not show a systematic energy-dependence in the energy range from 0.4 to 3.5 MeV within statistical uncertainties of 2.0 per cent (51).

The Li-Glass Detector

Li-glass detectors are often applied in measuring neutron fluxes utilizing the reasonably well known $^{6}Li(n,\alpha)T$-cross section. For the present measurements a 0.1 cm thick, 1.9 cm radius lithium glass was used. The glass was mounted on the axis and at the face of a cylindrical chamber with two or four multipliers viewing the scintillation light through air. This "free" mounting avoids corrections for effects due to scattering in light conductors and multipliers. A detailed Monte Carlo evaluation of the neutron scattering in the Li-glass was carried out and described elsewhere (56).

DATA ACQUISITION

The majority of the data were analyzed and recorded with an on-line-computer system (57). The time-of-flight spectra were recorded with one nsec-channel width. The energy spectrum corresponding to the (monoenergetic) neutron peak in the time-of-flight spectrum and that from an adjacent equally spaced interval from the time-of-flight spectrum were recorded.

The signals from both detectors were fed through the same data-input terminal using a tag for detector identification. This causes any dead-time effects to cancel as the computer software imposes the predominant dead-time of the data acquisition system.

MEASUREMENTS OF THE CROSS SECTION SHAPE

A cross section is characterized by its shape and absolute amplitude. In most experiments some systematic uncertainties apply to all values (for example mass-assignment, detector calibration, etc.), thus, it is justifiable to separate the shape measurement from the absolute measurement. This approach is usually made in cross section measurements with "white neutron sources" where the shape is measured using a cross section with a well known energy-dependence, usually $\sim 1/\sqrt{E}$. The resulting values are normalized to the thermal cross section or resonance parameters. In other experiments the shape of a cross section is measured using a neutron detector with a smooth and flat efficiency. Such measurements were previously carried out for the determination of capture cross sections using the Grey Neutron Detector (58,59). However, an "open geometry" was used in the present experiment for the fission counter to overcome the tremendous count rate problem with a collimated neutron beam. This solution was applied in recent measurements by Szabo et al. (25).

Measurements of the cross section shape were carried out using all three neutron detectors described above. The energy ranges, detectors and the foils used in the experiments are summarized in Table III.

Measurements using the BND as Monitor

The experimental setup is shown in the schematic in the upper part of Fig. 9. The fissile sample (S-2π-2) was placed in the fast-timing ionization chamber (FT-IC) about 10 cm away from the target. The collimator (40 cm long, 1.25 cm diameter cylindrical hole), was located at a distance of about 6.2 m from the target. The smaller Black Neutron Detector was positioned at a distance of about 7.1 m from the target. A neutron detection effective cutoff energy of $\sim$ 275 keV was determined by the observation of the time-of-flight spectra as a

function of the primary neutron energy. Data were measured in the energy range 400 - 2800 keV using about ± 20-30 keV incident neutron energy resolution for most of the measurements. However, a resolution of about ± 12 keV was used in the region near 900 keV where the fission cross section of ^{235}U shows a significant sharp rise with energy.

The fission count rate was obtained from the peak in the fission detector time-of-flight spectrum which had a resolution of about 4 nsec. The threshold was set well above the α-detection threshold. The neutron count rate was obtained from the integration of the neutron peak in the neutron detector time-of-flight spectra. Some additional background was subtracted due to counts found outside the energy range in which they must be expected for the Black Neutron Detector energy sum-spectrum. The statistical uncertainty of the raw data was less than 1 per cent. The reproducibility was checked at several energies and found to be within the statistical limits of the measurements.

Corrections were applied for several energy dependent effects as summarized in Table IV. In this table the range of the corrections and the uncertainties they contribute to the final results, are given. The major corrections were for the efficiency of the BND, the transmission through air and the fission counter walls, and for the second neutron group of the neutron source reaction. A ten per cent uncertainty was assumed for the total cross sections involved in the evaluation of the transmission through air and the fission counter walls. This may be a rather high estimate between resonances but appears appropriate at the resonances of the respective cross sections. At the fission detector, the second neutron group was not separated at most of the energies with the time-of-flight technique, but it was separated with the neutron detector. The uncertainty of the required correction is determined by the uncertainty of the yield ratio of the second to the first neutron group of the $^{7}Li(p,n)^{7}Be$-source reaction (error less than 5 per cent) and the ratios of the fission cross sections at the

appropriate energies (error less than 5 per cent).

The correction for fission events due to neutrons scattered elastically and inelastically in the target and the counter structure was evaluated by taking into account the cross sections of the materials involved, the angular distribution of the source reaction and of the scattering cross sections, and the effective thickness of the scattering material and the fissile sample for the primary and scattered neutrons. Analytical and Monte Carlo techniques were used in these evaluations.

The fission foil subtended an angle of ± 7 degrees with respect to the neutron source whereas the neutron detector measured essentially the zero degree neutron yield. Thus a correction was applied for the angular distribution of the neutron source using a two term expansion, $Q = A_{11} + A_{12} \cdot \cos\theta$, with the coefficients A_{11} and A_{12} taken from Ref. 36.

Neutrons leaking out of the BND without collision or with collisions involving only carbon may be scattered in the surrounding shielding material and return within the time-resolution of the detector. The correction was estimated from the cross sections of the materials involved and the solid angle subtended by the BND for backscattered neutrons. The transmission through the collimator was extensively treated in Ref. 60. This correction is small due to the large distance of the collimator from the neutron source.

Results obtained in the measurements for the shape of the fission cross section of U-235 described above are given in Table V and are shown in Fig. 10. The values were normalized to absolute values as described below. The uncertainties given for the cross sections in Table V are at the 68 per cent confidence level and do not contain the uncertainty of the normalization. The energy resolution is given in the Table.

The first value (at 399 keV) has limited validity because at this energy the efficiency of the BND drops off sharply due to the light detection cutoff. Average values, rounded to millibarn were given when two values were available at the same or very similar energy (±.2 keV).

Shape Measurements with the GND as Flux-Monitor

The experimental setup is shown in the lower part of Fig. 9. A gas scintillation counter (2π-GSC) was positioned 10 to 20 cm away from the target. The collimator was positioned at a distance of about 50 cm from the source and the neutron beam was monitored with the Grey Neutron Detector placed at a distance of 3.8 m from the neutron target.

Measurements were carried out in the energy range from 35 keV to 3.5 MeV. Some measurements were carried out at a 60° angle from the direction of the primary proton beam, however, most measurements were made at 0°. Energy resolution varied from ± 3 keV to ± 70 keV. The fission fragment energy spectra and the time-of-flight spectra for the fission counter and the energy spectra of the GND were recorded with the on-line computer system. The fission fragment energy spectra was used to monitor the stability of the fission counter, and the fission count rate was obtained from the time-of-flight spectra. The threshold was set at about 40 MeV in order to exclude all background caused by fast neutrons in the scintillation gas, in the multipliers and the structural material.

The neutron-detector count-rate was obtained from the γ-ray spectra by integrating the appropriate ranges, as indicated in Fig. 8. The Background of the Grey Neutron Detector was determined in separate runs with a plugged collimator hole. With these measurements, background from room-scattering and leakage through the detector shielding was eliminated. Background independent of the $^{7}Li(p,n)^{7}Be$-neutron source was determined with an empty target cup and found to be negligible.

Several corrections were applied which were similar to those discussed for the measurements with the BND. However, some of the major corrections were reduced (second neutron group, scattering in the fission counter) or of a different nature (efficiency of the neutron detector). The largest corrections were again for the transmission of the primary neutron beam through the fission counter wall and the air between the fission counter and the neutron monitor. The counter wall consists of iron and the transmission was in the range of 98.4 to 99.1 per cent, except in some resonances where it was as low as 91.3 per cent. However, only a few points were measured at energies coincident with large resonances in the iron cross section. The correction for transmission through air was in the 1.5 - 4.3 per cent range, except around 430 keV where the resonances in oxygen and nitrogen cause a correction up to 8.5 per cent. Neutrons scattered in the molybdenum-backing of the fissile sample require a correction which is mainly due to the loss of neutrons detected by the neutron counter. The loss of neutrons passing the fissile sample is compensated for, in part, by an increase of the effective foil thickness for these neutrons scattered into the fissile sample.

The second neutron group of the $^{7}Li(p,n)^{7}Be$-reaction contributes up to 11 per cent to the total neutron yield, however, the cross section of the $^{235}U(n,f)$-reaction does not change more than 10 per cent in the range where the second neutron group contributes significantly to the fission rate, and the efficiency of the neutron detector differs by only up to 3 per cent for the two groups. The total correction for the second neutron group does not exceed one half per cent because the second neutron group is not separated by the time-of-flight technique with either detector. The correction required for scattering of neutrons in the target backing and target assembly is of a similar nature. These scattering events cause an additional non-monoenergetic component in the neutron beam. The correction was evaluated using the known angular distribution of the source reaction, the thickness of the tantalum backing, the energy-

dependence of the fission cross section and neutron detector efficiency. In-scattering of neutrons from the collimator has been considered previously (58). In the present experiment this background was estimated to be less than 0.1 per cent. The scattering in the walls and other structural material of the fission counter caused only a small correction for the 2π-gas scintillation counter because of its large size. The total correction applied for the experiment with the GND is shown as a function of energy in Fig. 11.

The results from the present shape measurements are given in Table VI and are shown in Fig. 12. The shape values were normalized with the results from the absolute measurements as discussed below. The statistical uncertainty contributed significantly to the error of the measurements with the GND (1.5 - 3.5 per cent). Other contributions are from the uncertainty of the corrections (0.5 - 2.0 per cent) and from the energy-dependence of the neutron detector efficiency. The contribution from the latter increases with energy to a $\sim$2 - 3 per cent uncertainty, which is the limitation for the shape measurements with the GND above 1.5 MeV. Some values shown in Fig. 12 are averages as given in Table VI. The nearest whole keV and millibarn were quoted.

Measurements with the Li-Glass Detector

Measurements with the GND become increasingly difficult at lower energies due to the low neutron intensity of the source reaction. Thus the measurements with the GND were supplemented with shape measurements in the energy range below 110 keV utilizing the ^{6}Li(n,α)T cross section for neutron flux monitoring.

The fission detector and the Li-glass detector were positioned back to back at an angle of 77° to the incident proton beam direction. The fission foil and the lithium glass were on opposite sides of the counters, the former about 13 cm from the target and the latter about 25 cm.

Data were taken in the energy range from 35 to 110 keV and one point at 250 keV. The count rate was obtained from the peak in the time-of-flight spectrum subtracting the background from an equally spaced interval adjacent to the peak.

Corrections were applied for transmission through counter walls and scattering of neutrons in the target and counter material as discussed above. Recent measurements of the $^{6}Li(n,\alpha)T$ cross section resulted in consistent ratios for the peak of the resonance to the "valley"-value between 90 and 100 keV (33). The data used for the $^{6}Li(n,\alpha)T$ cross section are based on these measurements and are listed in Table VII. Only the shape of the present measurements was used and the ^{235}U fission cross section values were normalized at 250 keV to the results obtained with the GND.

The results are listed in Table VII and shown in Fig. 12. The major uncertainties are from the normalization procedure (2.0 per cent) and the statistics (1.5 - 2.0 per cent).

ABSOLUTE CROSS SECTION MEASUREMENTS

Absolute measurements were carried out at energies favorable for the respective technique. Thus, absolute measurements with the BND were carried out at 3.5 MeV (using the larger detector) and at 0.3 MeV (using the smaller detector) in order to have sufficiently higher energies than the cutoff in the efficiencies and a small correction for secondary effects. The associated activity technique was employed in the 450 - 650 keV energy range because the fission cross section does not vary much with energy in this region and therefore the energy spread of the $^{51}V(p,n)^{51}Cr$-reaction introduces only a minor uncertainty of the cross section result. Finally, the measurement with the calibrated vanadium bath was carried out at 500 keV neutron energy because the

peak in the neutron yield of the source reaction $^{7}Li(p,n)^{7}Be$ helps to overcome count rate problems.

Table VIII summarizes the absolute measurements, indicating the uranium foils and fission detectors used, and the neutron flux measurement techniques which were applied in the experiments.

Measurements Using the BND

The Black Neutron Detector has an efficiency close to one, thus, 10^{6} higher than the reaction-rate of a typical fission foil used to measure the fission cross section. A 1000 cps rate is reasonable with the electronic and computer equipment; this count rate corresponds to about 1000 neutrons per second measured with the Black Neutron Detector. A 500 $\mu g/cm^{2}$ uranium foil would yield about 6 fissions per hour in this beam. In order to reconcile both efficiencies, a double collimator system was used in the present experiment with the larger BND. An open geometry for the fission foil and a collimator for the neutron detector were used with the smaller BND.

The absolute measurements were carried out at 0.8 MeV and 3.5 MeV neutron energy. In the experiment with the larger BND at 3.5 MeV, a neutron beam was first collimated in such a way that the entire deposit of the 4π-uranium sample positioned in the fission counter at a 173-cm flight path was radiated, but not the structural material of the scintillation chamber. A second collimator provided for a lower intensity beam for the Black Neutron Detector which was positioned 440 cm behind the target. The experimental setup is shown in the schematic in Fig. 13.

The threshold for recording fission events was set below the α-detection threshold, and the spectra contained background not only from fission events caused by straying low-energy neutrons but also of alphas and effects from

(n,x)-reactions as well. The count rate was obtained from the fission spectra coincident with the neutron peak in the time-of-flight spectrum. Background was eliminated by subtracting the energy spectra obtained for an equally spaced range in the time-of-flight spectrum adjacent to the neutron peak.

The existance of additional background in the range of the fission spectra was checked by a measurement without the fissile sample. The total background amounted to 13 per cent of the count rate. The spacial distribution of the neutron yield in forward-direction after the first collimator is assumed isotropic. This assumption is well justified due to the small opening angle subtended by the uranium foil (0.8 degree). The neutron flux per cm^2 hitting the uranium foil is measured with the neutron detector after the second collimator, thus the opening angle of the collimator is needed. This is determined by the exit opening of the collimator, the distance between the neutron source and the collimator, and the transmission through the side of the collimator channel. The present collimator was 40.6 cm long with a cylindrical channel whose cross sectional area was about 0.33 cm^2, determined from samplings of the diameter and volume measurements. Due to the large distances from the second collimator to the neutron source and from the collimator to the detector, the correction for transmission through the collimator and scattering into the neutron detector is small.

For the measurement at 0.8 MeV with the smaller BND a thinner ^{235}U foil was used in open geometry. The setup is similar to that shown for the shape measurements in Fig. 9. The uranium foil (S-2π-4) was positioned in the fast-timing ionization chamber at a distance of about 9 cm from the target. A cylindrical collimator with an opening diameter of about 1.3 cm provided a low intensity neutron beam for the BND which was positioned at a distance of about 7 m from the target.

The corrections required for both measurements are summarized in Table IX. These corrections are similar to those applied to the shape measurements and were discussed in the appropriate sections. The uncertainties which are caused by these corrections and contribute to the results are also given in Table IX. The results obtained for the absolute cross sections are

$$\sigma_f(800 \text{ keV}) = (1134 \pm 27)\text{mb}$$

$$\sigma_f(3500 \text{ keV}) = (1198 \pm 26)\text{mb}$$

Absolute Measurements Using the Associated Activity Technique

The absolute neutron source strength of a (p,n)-reaction may be determined from the residual nuclei if such nuclei are radioactive. This technique was employed in the past for measuring (p,n)-reaction cross sections, calibrating neutron detectors and measuring absolute neutron cross sections (61-64, 55). The $^{51}V(p,n)^{51}Cr$-reaction was used in the present experiments. Measurements were carried out in energy regions with only a small change of the fission cross section over the spectra range of the neutron source.

The setup for the experiment is shown in Fig. 3. The proton beam is collimated by gold aperatures and strikes the target in the center of the spherical fission counter. The pulse height spectra of the fission fragments obtained from the spherical ionization chamber is recorded with a multichannel-analyzer. The number of fission events during the irradiation is obtained by extrapolating this spectrum to zero pulse height and correcting for total fission fragment absorption. After the irradiation, which lasted 100-600 min., the γ-activity of the target was measured 2-3 times with a NaI(Tl)-detector. The γ-ray spectra was recorded with a multichannel-analyzer and the photopeak at 320 keV from the decay of ^{51}Cr was used. The NaI(Tl)-detector was calibrated with absolutely measured ^{51}Cr-sources supplied by the EURATOM- and CHALK RIVER-laboratories. The calibration factor includes the photopeak efficiency of the detector and the

branching ratio of the decay of ^{51}Cr. An additional value may be obtained from the photopeak efficiency of the detector and the branching ratio as reported in the literature (65). However, this results in a rather uncertain value and does not influence the calibration factor. The calibration values are shown in Fig. 14.

Measurements were carried out in the neutron energy range from 448 to 650 keV using three different spherical fission counters. Two sources of background were identified and determined experimentally. Fission events due to neutrons produced by protons hitting beam tubes, aperatures or the target backing were determined by measurements with an "empty" target. This background was found to be 1 - 2 per cent. Neutron background scattered by the environment (laboratory walls, floor and beam tube support) usually is determined utilizing the $1/r^2$-law of the primary neutron flux. This technique was also applied in the present experiments. However, the background was determined by measuring in different directions from the source and using an appropriate average. This background was in the order of 1 - 5 per cent of the count rate, the smaller amount applying to a laboratory with the walls and the floor more than 3 m away, the larger number for a laboratory with only 1.1 m to the floor and the wall.

The corrections applied in the present experiment are summarized in Table X. Primary neutrons which are scattered in the spherical detector or the target assembly cause an increase in the fission rate. This increase is due primarily to the longer flight path through the fissile deposit for neutrons scattered before they reach the ^{235}U layer, and due to the increase of the neutron flux by neutrons backscattered after they passed the ^{235}U layer. The largest correction is due to neutrons scattered in the inner sphere on which the uranium is deposited. The increase of the path-length through the uranium layer was previously evaluated assuming isotropic scattering from silver (26). However, because this correction is the largest to be applied, a Monte Carlo evaluation was carried out taking

into account the angular distribution of the neutron scattering on Ag. A correction of 2.5 per cent was obtained from this evaluation for the Ag 10 detector and 4.2 per cent for the Ag 20 detector. The difference between the result from the analytical evaluation and the result from the Monte Carlo technique was small (0.2 per cent).

The scattering at the outer sphere increases the neutron flux at the inner sphere with the uranium deposit. In addition each scattered neutron hitting the inner sphere passes the uranium layer twice, thus amplifying the effect. Scattering in all other target and detector structural material causes similar additional fission events. These corrections are in general small and were estimated by evaluating the amount of scattering, the space angle subtended by the uranium-deposit to the scattering source, and the effective thickness of the ^{235}U layer for the scattered neutrons. The energy change of the neutrons due to inelastic scattering was taken into account for scattering in the target backing only because the total amount of scattering on all other material is small. The results from the present measurements are listed in Table XI.

Measurements with a Calibrated Vanadium Bath

A vanadium bath (66) was used for an absolute measurement at 500 keV neutron energy. Although this technique may be applied as an absolute technique like the manganese bath technique, the present vanadium bath was calibrated with Cf-sources. The same vanadium-sulfate solution and tank used for the GND were also used in this experiment.

Two calibration values were obtained, one by using an absolutely calibrated ^{252}Cf-source (67), and another by using a ^{252}Cf-deposit for which the spontaneous fission decay rate was measured with a surface barrier detector in a low geometry counter. The neutron emission for the latter was obtained from the spontaneous

fission decay rate and the known value for the number of neutrons per fission event, $\bar{\nu}$ (33).

The calibration value obtained with the absolutely calibrated ^{252}Cf-source was determined by irradiating the vanadium bath with the ^{252}Cf-source and then measuring the 1.4 MeV γ-ray from the decay of ^{52}V with a NaI-detector at the surface of the bath. The same procedure was repeated with 500 keV neutrons from the ^{7}Li(p,n)T-reaction, however, the 2.2 MeV γ-ray from the capture in hydrogen during the irradiation was recorded. Comparison of the vanadium-activities and the known Cf-source strength yields the calibration factor for the detection of prompt 2.2 MeV capture γ-rays at 500 keV neutron energy.

A second calibration value was obtained from the ^{252}Cf-source with the measured spontaneous fission rate. In this case the 2.2 MeV capture γ-ray was directly detected during the irradiation with the source. In order to obtain the efficiency for 500 keV neutrons the average of the detector efficiency over the fission spectra of ^{252}Cf (68) was evaluated. Because of this correction and the higher background, this technique resulted in a calibration value with a larger uncertainty.

Corrections were applied for the leakage of neutrons from the vanadium bath (0.7 per cent at 500 keV and 1.4 per cent for the ^{252}Cf-source) (69, 70) and the absorption in the source and channel material (0.2 per cent). The latter was determined by doubling the amounts of materials involved.

The corrections used for the vanadium bath relied upon the extensive investigations by DeVolpi and Porges (71, 72). This appears appropriate as the calibrated ^{252}Cf-source was obtained from the same experimenters. The two values obtained from these calibration procedures are

$$\eta_1(500\ \text{keV}) = (1.305 \pm 0.030)\ .\ 10^{-4}$$

$$\eta_2(500\ \text{keV}) = (1.318 \pm 0.040)\ .\ 10^{-4}$$

and the weighted average $1.310\ 10^{-4}$ was used.

The setup for the measurement of the ^{235}U fission cross section at 498 keV with the calibrated vanadium bath is shown in Fig. 13. The advantage of this measurement at 498 keV is that many of the required corrections were eliminated. However, the count rate for the fission counter was very low and a long irradiation time was required ($\sim$ 2 days).

The same fission counter and uranium deposit were used as in the measurement with the BND at 3.5 MeV. Corrections were applied for the transmission through the counter and the air, as well as for scattered neutrons, as discussed before. The value

$$\sigma_f(498\ \text{keV}) = (1151 \pm 42)\text{mb}$$

was obtained. The major contributions to the uncertainty of this result were from the calibration of the vanadium bath (2.3 per cent) and from the statistics for the fission counting (also 2.3 per cent). Other contributions were from the fission counting efficiency (1.0 per cent), the uranium mass (0.5 per cent), the limit on the homogenuity of the uranium distribution on the sample (1.0 per cent) and for corrections (0.5 per cent).

RESULTS AND DISCUSSIONS

It should be emphasized that the values given in Tables V, VI and VII are the results for the shape of the cross section and may be multiplied by any factor desirable. However, the numbers as quoted in the tables were normalized with absolute values obtained in the present experiments in order to quote cross section values. The shape values measured with the BND were normalized with the absolute value obtained at 800 keV with the small BND. The shape values measured

with the GND were normalized with the absolute value obtained with the calibrated vanadium bath, and the values obtained relative to the $^{6}Li(n,\alpha)$ cross section shape were normalized in turn to the GND values at 250 keV.

A final result of average values for the fission cross section over the entire energy range from 35 to 3500 keV was obtained by evaluating an average shape of the cross section from the data in Tables V, VI and VII, and normalizing this shape with all the absolute values obtained in the present measurements. For this purpose, eye-guide curves were drawn through the results of the three different shape measurements. These shape curves were normalized at small overlapping energy ranges to the same value and a weighted average for the shape of the cross section in the total energy range was evaluated. This shape was normalized with the absolute values by minimizing the differences between the absolute values obtained from the three different techniques and the shape result. This final result from the present measurements is given in Table XII.

The final result is also shown in Figs. 10 and 12. A ± 3 per cent uncertainty range is indicated in Figs. 10, 12 and 15. This error range was assumed as the uncertainty of the present measurements from the different measurements and the agreement between the independent results. Besides some fluctuations which must be expected from the statistical contributions to the uncertainties of the single points the agreement between the results from different techniques is well within the uncertainty range of the present measurements. The results as given in Table XII smooth out statistical fluctuations but also may ignore some real structure which is smaller than the present uncertainty range. However, structure of less than 2 per cent in the energy range above 100 keV should be of no concern for reactor purposes. Structure in the fission cross section of ^{235}U below 100 keV, as known from other measurements (77), may be superimposed on the present average values.

The results obtained with the GND for the shape of the cross section are somewhat higher in the energy range above 1 MeV than the values obtained with the BND. The difference is systematic but well within the uncertainty limits. The measurements with the BND should be more reliable in this energy range. On the other hand, the agreement in the overlap-range above 500 keV suggests that the GND-shape results obtained below 500 keV should be reliable within their uncertainty range. The efficiency of the GND is much flatter in this lower range than in the MeV range.

The present results as given in Table XII are compared with values obtained by other experimenters in Fig. 16. Only the more recent results (later than 1965) and available for reference were compared with the present measurements. Older measurements are, with few exceptions, up to a factor two higher and were displayed at other occasions (26, 29). Fig. 16 shows good agreement between these data within their respective uncertainty ranges. A possible exception are some of the values by White (20) in the lower energy range and by Kaeppeler (73).

The average of the fission cross section of ^{235}U over the fission spectrum of the ^{252}Cf-spontaneous fission process provides a first check of the integral quality and normalization of the present results. The advantage of this average over other integral (reactor) quantities as a test of the fission cross section of ^{235}U is its independence on other nuclear data, including the average energy of the Cf-spectrum. Using the Maxwellian spectrum

$$\phi\,(E) \sim E \exp - \frac{E}{\frac{2}{3} E_a}\,, \quad E_a = 2.2 \text{ MeV}$$

a change of only ± 0.2 per cent is caused by a change of E_a by ± 10 per cent. Similarly, the difference obtained for the average cross section is only 0.5 per cent if the cross section of ^{235}U outside the range of the present measurements is changed between its extreme possible limits. Thus, the average of the

fission cross section of ^{235}U over the ^{252}Cf fission spectrum depends essentially only on the absolute values of the differential cross section.

The result for the average of the present measurements over above spectrum is 1.230 barn. This compares well with a measurement by Grundle (78) of 1.207 ± 0.052 barn and by Dorofeev and Dobrynin (6) of 1.22 ± 0.08 barn. The latter is an average over a mock-fission source spectrum.

Acknowledgement

The 4π-fission foils were supplied by EURATOM, Geel. ^{51}Cr calibration samples were supplied by the RURATOM and by the Chalk River Laboratories. Dr. Meadows was helpful with previously unpublished data on the α- and fission fragment absorption. A calibrated ^{252}Cf-source was obtained from Dr. DeVolpi.

References

1. A. O. Hanson, "A Measurement of Fission Cross Sections by the Use of a Coincidence Proportional Counter", USAEC Report CF-628, University of Wisconsin, April 1943.
2. D. L. Benedict and A. O. Hanson, "Final Report on a Measurement of the 25 Cross Section for 0.53 MeV Neutrons by the Manganese Solution Method", USAEC Report CF-638, University of Wisconsin, April 1943.
3. P. G. Koontz, T. A. Hall, and B. Rossi, "Absolute Values of the Fission Cross Sections of 25 and 28 from 0.28 to 2.5 MeV", USAEC Report LA-128, Los Alamos, Scientific Laboratory, August 23, 1944.
4. J. H. Williams, "The Cross Sections for Fission of 25, 49, 28, 11, 37, 00, 02, B and Li", USAEC Report LA-150, Los Alamos Scientific Laboratory, Oct. 5, 1944.
5. C. L. Bailey, "Fission Cross Section of ^{235}U from 20 to 500 keV", USAEC Report LA-447, Los Alamos Scientific Laboratory, Nov. 20, 1945.
6. G. A. Dorofeev and Y. P. Dobrynin, "Effective Fission Cross Sections of ^{233}U, ^{235}U, ^{239}Pu and ^{240}Pu in the Neutron Energy Range 30 keV - 5 MeV", J. Nucl. Energy 5, 217 (1957).
7. R. L. Henkel, "Summary of Neutron Induced Fission Cross Sections", Los Alamos Scientific Laboratory, LA-2114 (1957).
8. W. D. Allen and A. T. G. Ferguson, "The Fission Cross Sections of ^{233}U, ^{235}U, ^{238}U, and ^{239}Pu for Neutrons in the Energy Range 0.030 - 3.0 MeV", Proc. Phys. Sco. A70, 753 (1957).
9. B. C. Diven, "Fission Cross Section of ^{235}U for Fast Neutrons", Phys. Rev. 105, 1350 (1957).
10. R. L. Henkel, "Fast Neutron Cross Sections", USAEC Report LA-2122, Los Alamos Scientific Laboratory, Mar. 1, 1957 and R. L. Henkel, "Fast Neutron Cross Sections: Corrections to LA-1714 and a Correlation of 3 MeV Values", LA-2122 (1957), also, R. L. Henkel, "Fission Excitation Curves for ^{233}U, ^{235}U, ^{236}U and ^{237}Np", Los Alamos Scientific Laboratory, LA-1495 (1952).
11. D. Szteinsznaider, V. Naggiar, and F. Netter, "Energy Dependence of ^{233}U, ^{235}U, ^{239}Pu Fast Neutron Cross Sections", Peaceful Uses of Atomic Energy (1955), P/355, Proc. Vol. 4, P. 245.

12. S. P. Kalinin and V. N. Ponkratov, "Neutron Induced Fission Cross Sections of Th-232 and U-238 in the Energy Range 3-11 MeV", Geneva Conf. on Peaceful Uses of Atomic Energy (1958), P/2149, Proc. Vol. 16, p. 136.

13. E. Melkonian, V. Perez-Mendez, M. L. Melkonian, W. W. Havens, Jr., and L. J. Rainwater, "Slow Neutron Velocity Spectrometer Studies of the Total and Fission Cross Sections of ^{235}U", Nucl. Sci. Eng. 3, 435 (1958).

14. V. M. Pankratov, "Fission Cross Sections of ^{232}Th, ^{233}U, ^{235}U, ^{237}Np and ^{238}U for 5 - 37 MeV Neutrons", J. Nucl. Energy A/B, React. Sci. Techn. 18, 215 (1964).

15. M. L. Yeater, P. L. Kelley, and E. R. Gaerttner, "A High Resolution Measurement of the Fission Cross Sections of ^{235}U", USAEC Report KAPL-1109, Knolls Atomic Power Laboratory, 1954.

16. F. Metter, "Some Aspects of the Nuclear Fission Process", Report CEA-1913, Commissariat a l'Energie Atomique, France, 1961.

17. A. Michaudon, R. Genin, R. Joly and G. Vendryer, "Measurements of Fission Cross Sections and Number of Prompt Neutrons Emitted during Fission", Proc. 1958 Geneva Conf. 16, Paper No. 1186, p. 106.

18. G. V. Gorlov, B. M. Goshberg, V. M. Morozov, G. A. Ostroshehenko and V. A. Shigin, "The Fission Cross-Sections of ^{233}U and ^{235}U for Neutrons Having Energies between 3 and 800 keV", J. Nucl. Energy 12, 79 (1960).

19. G. N. Smirenkin, V. G. Nesterov and I. I. Bondarenko, "^{233}U, ^{235}U and ^{239}Pu Fission Cross Sections for 0.3 - 2.5 MeV Neutrons", Atomnaya Energiya 13, 366 (1962).

20. P. H. White, "Measurements of the ^{235}U Neutron Fission Cross Section in the Energy Range 0.04 - 14 MeV, J. Nucl. Energy A/B 19, 325 (1965).

21. J. L. Perkin, P. H. White, P. Fieldhouse, E. J. Axton, P. Cross and J. C. Robertson, "The Fission Cross Sections of ^{233}U, ^{234}U, ^{235}U, ^{237}Np, ^{239}Pu, ^{240}Pu and ^{241}Pu for 24 keV Neutrons", J. Nucl. Energy 18, 423 (1965).

22. G. F. Knoll and W. P. Poenitz, "A Measurement of the ^{235}U Fission Cross Section at 30 keV and 64 keV", J. Nucl. Energy 21, 643 (1967).

23. W. P. Poenitz, "Measurement of the ^{235}U Fission Cross Section in the keV Energy Range", Proc. Second Conf. on Neutron Cross Sections and Technology, Washington, D. C., 1968, NBS Special Publication 299, Vol. I, p. 503, Conf. 680307.

24. R. K. Smith, R. L. Henkel and R. A. Nobels, "Neutron Induced Fission Cross Sections for ^{233}U, ^{235}U, ^{238}U and ^{239}Pu from 2 to 10 MeV", Bull. Am. Phys. Soc. 2, 196 (1957) Revised values.

25. I. Szabo, J. P. Marquette, E. Fort and J. L. Leroy, "Mesure Absolute de la Section Efficace de Fission", Proc. IAEA Conf. on Nucl. Data for Reactors, Helsinki, 1970, CN-26/69, and
I. Szabo, G. Filippi, J. L. Huet, J. L. Leroy and J. P. Marquette, "New Absolute Measurements of the Neutron-Induced Fission Cross Section of ^{235}U, ^{239}Pu and ^{241}Pu from 17 keV to 1 MeV, see Ref. 32, p. 257, and
I. Szabo, G. Filippi, J. L. Huet, J. L. Leroy and J. P. Marquette, ^{235}U Fission Cross Section from 10 keV to 200 keV", Proc. of 3rd. Conf. on "Neutron Cross Section and Technology", CONF-710301, p. 573 (1971).

26. W. P. Poenitz, "Measurements of the ^{235}U Fission Cross Section at 552 and 644 keV", see Ref. 32, p. 281.

27. J. R. Lemley, G. A. Keyworth, and B. C. Diven, "High Resolution Fission Cross Section at ^{235}U from 20 eV to 100 keV", Nucl. Sci. and Eng. 43, 281 (1971).

28. F. Kaeppeler, "Measurement of the Fission Cross Section of ^{235}U at 440 and 530 keV Neutron Energy", see Ref. 32, p. 272.

29. W. P. Poenitz, "Interpretation and Intercomparison of Standard Cross Sections", see Ref. 32, p. 331.

30. Symposium on the "Absolute Determination of Neutron Flux in the Energy Range 1 - 100 keV", Oxford 1963, European American Nuclear Data Committee, EANDC-33"U".

31. Panel on "Nuclear Standards for Neutron Measurements", Brussels 1967, International Atomic Energy Agency, IAEA-107.

32. Symposium on "Neutron Standards and Flux Normalization", Argonne 1970, Argonne National Laboratory, USAEC Symp. Series 23, CONF-701002.

33. Second Panel on "Neutron Cross Section Reference Data", Vienna 1972, International Atomic Energy Agency, Proc. to be published.

34. J. H. Gibbons and H. W. Newson, "The $^{7}Li(p,n)^{7}Be$-Reaction", in "Fast Neutron Physics", Edited by J. B. Marion and J. L. Fowler, Inters. Publ., Inc. 1960, p. 133.

35. P. R. Bevington, W. W. Rolland, and H. W. Lewis, "Relative Yield of Neutron Groups from the $^{7}Li(p,n)^{7}Be$, $^{7}Be^{*}$ Reactions", Phys. Rev. 121, 871 (1961).

36. J. W. Meadows, and D. L. Smith, "Neutrons from Proton Bombardment of Natural Lithium", Argonne National Lab., ANL-7938, 1972.

37. G. Deconninck, and J. Royen, "La Reaction $^{51}V(p,n)^{51}Cr$ Comme Source De Neutrons Monoenergetiques", Nucl. Instr. and Methods 75, 266 (1969).

38. Ch. M. Huddleston, "Gaseous Scintillation Detectors", and R. W. Lamphere, "Fission Detectors", in "Fast Neutron Physics", edit. by J. B. Marion and J. L. Fowler, Int. Science Publ., Inc. 1970, p. 441 and p. 449.

39. W. P. Poenitz, "Measurement of the Ratios of Capture and Fission Neutron Cross Sections of ^{235}U, ^{238}U, and ^{239}Pu at 130 to 1400 keV", Nucl. Science and Eng. 40, 383 (1970).

40. J. W. Meadows, "The ^{238}U to ^{235}U Fission Cross Section Ratio from 1 to 5 MeV", Nucl. Sci. Eng. 49, 310 (1972).

41. J. W. Meadows, "The Alpha Half-Life of ^{234}U", Argonne National Laboratory, ANL 7610, 1969.

42. M. Lounsbury and R. W. Durham, "The Alpha Half-Life of ^{234}U", Conf. on Chemical Nucl. Data, Canterbury 1971, British Nucl. Energy Soc., p. 48.

43. P. H. White, G. J. Wall and F. R. Pontet, "A Remeasurement of the Half-Life of ^{235}U", J. Nucl. Energy A/B 19, 33 (1965), and references cited therein.

44. J. W. Meadows, Argonne National Laboratory, Private Communication (1973).

45. G. W. Knobeloch, "Precision Assay by Fission Counting", European-American Nuclear Data Committee, EANDC-53 (S) p. 363 (1966).

46. A. J. Deruytter, "Precise Low-Energy Fission Cross Sections", see Ref. 32, p. 221.

47. J. W. Meadows, Argonne National Laboratory, Private Communication (1973).

48. J. E. Perry, Jr., "Neutron Flux Measurements", in "Fast Neutron Physics", Edit. by J. B. Marion and J. L. Fowler, Interscience Publ., Inc. p. 623 (1960).

49. A. T. G. Ferguson, "Gas Recoil Counters", and C. D. Schwartz, and G. E. Owen, "Recoil Detection in Scintillators", and C. H. Johnson, "Recoil Telescope Detectors", in "Fast Neutron Physics", Edit. by J. B. Marion and J. L. Fowler, Interscience Publ. Inc. p. 179 ff. (1960).

50. W. P. Poenitz, "The Black Neutron Detector", Argonne National Laboratory, ANL-7915 (1972).

51. W. P. Poenitz, "Two Flat Response Detectors for Absolute and Relative Neutron Flux Measurements", see Ref. 33.

52. W. P. Poenitz, "The Black Neutron Detector", Nucl. Instr. and Method, to be published (1973).

53. W. P. Poenitz and E. Wattecamps, "A Grey Neutron Detector for Flux Measurements in the Intermediate Energy Range", see Ref. 30, p. 102.

54. W. P. Poenitz, "A Grey Neutron Detector for the Intermediate Energy Region", Nucl. Instr. and Methods 58,39(1968).

55. W. P. Poenitz, "Experimental Determination of the Efficiency of the Grey Neutron Detector", Nucl. Instr. and Methods 72, 120 (1969).

56. W. P. Poenitz and J. W. Meadows, "The ^{6}Li(n,α)T Cross Section", to be published (1973).

57. W. P. Poenitz and J. F. Whalen, "On-Line Computer Facility and Operating System COSACS at the ANL Fast Neutron Generator", Argonne National Laboratory, to be published (1973).

58. W. P. Poenitz, D. Kompe, and H. O. Menlove, "The Neutron Capture Cross Section of Gold in the keV-Energy Region", J. Nucl. Energy 22, 505 (1968).

59. H. O. Menlove and W. P. Poenitz, "Absolute Radiative Capture Cross Section for Fast Neutrons in ^{238}U", Nucl. Sci. Eng. 33, 24 (1952).

60. J. L. Leroy, J. L. Huet, and J. Gentil, "Mesure des Flux Neutroniques D'Energie Comprise Entre 10 keV et 1 MeV Par La Methode du Bain de Manganèse, et Application a l'Etalomage d'un Compteur", Nucl. Instr. and Methods 88, 1 (1970).

61. R. Taschek and A. Hemmendinger, "Reaction Constants for ^{7}Li(p,n)^{7}Be", Phys. Rev. 74, 373 (1948).

62. R. C. Hanna and B. Rose, "Fast Neutron Capture in ^{238}U and ^{232}Th", J. Nucl. Energy 8, 197 (1959).

63. W. P. Poenitz, "The (n,γ) Cross Section of ^{197}Au at 30 and 64 keV Neutron Energy ", J. Nucl. Energy A/B 20, 825 (1966).

64. K. K. Harris, II. A. Grench, R. G. Johnson, F. J. Vaughn, J. H. Ferziger and R. Sher, "The ^{197}Au (n,γ) ^{198}Au Cross Section from 13 keV to 683 keV", Nucl. Phys. 69, 37 (1965).

65. Nuclear Data Sheets, National Academy of Sciences, Washington.

66. A. DeVolpi and K. G. Porges, "Advances in Accurate Fast Neutron Detection", NBS Special Publ. 299, Vol. 1, 213 (1968).

67. A. DeVolpi, Argonne National Laboratory (1972), Private Communication.

68. J. W. Meadows, "^{252}Cf Fission Neutron Spectrum from 0.003 to 15.0 MeV", Phys. Rev. 157, 1076 (1967).

69. D. R. Davy, "Neutron Escape from Manganese Sulfate Baths Used in the Calibration of Radioactive Neutron Sources", J. Nucl. Energy A/B 20, 277 (1966).

70. A. DeVolpi, "Neutron Escape from Water-Moderated Tanks", J. Nucl. Energy A/B 24, 577 (1971).

71. A. DeVolpi, and K. G. Porges, "Absolute Calibration of Neutron Sources Having a Wide Range of Emission Spectra", Metrologia 5, 128 (1969).

72. A. DeVolpi and K. G. Porges, "Neutron Yield of ^{252}Cf Based on Absolute Measurements of the Neutron Rate and Fission Rate", Phys. Rev. C.1, 683 (1970).

73. F. Kaeppeler, "A Measurement of the Neutron Fission Cross Section of ^{235}U between 0.5 and 1.2 MeV", see Ref. 33.

74. D. B. Gayther, D. A. Boyce, and J. B. Brisland, "Measurement of the ^{235}U Fission Cross Section in the Energy Range 1 keV to 1 MeV", see Ref. 33.

75. D. M. Gilliam, "An Absolute Determination of the ^{235}U Fission Cross Section at 964 keV", Dissertation, University of Michigan, 1973.

76. M. K. Drake, "ENDF/B-III Cross Section Measurement Standards", Brookhaven National Laboratory, BNL 17188 (1972).

77. C. D. Bowman, G. S. Sidhn, M. L. Stelts, and J. C. Browne, "Structure in the ^{235}U keV Fission Cross Section", Conf. on Neutron Cross Section and Technology, Knoxville, 1971, Vol. 2, p. 584, CONF - 710301.

78. J. A. Grundle, V. Spiegel, Jr., C. Eisenhauer, National Bureau of Standards, Private Communication (1972).

TABLE I. Physical Description of Fissile Samples.

Sample Label	Thickness in $\mu g/cm^2$	Area in cm^2	Fissile Material	Deposition Technique	Backing in cm	Used in Counter
S-2π-1	400	20	U-1	Electro-plating	Molybdenum 0.013	2π-GSC
S-2π-2	500	20	U-5	"	"	FT-IC
S-4π-400	400	19.63 ± 0.1	U-3	Electro-spraying	Vyns	4π-GSC
Ag-1	55	184.1 ± 1.1	U-1	Electro-plating	Silver 0.025	SS-IC-1
Ag-10	75	186.9 ± 1.1	U-2	"	"	SS-IC-2
Ag-20	60	189.6 ± 1.1	U-2	"	0.050	SS-IC-3
S-2π-4	100	5	U-4	Evaporation	St.Steel 0.025	FT-IC
S-2π-5	400	11	U-6	"	Molybdenum 0.013	2π-GSC

TABLE II. Isotopic Contents and Mass of the Fissile Samples.

Sample Label	Fissile Material	Isotopic Composition in wpc ^{234}U	^{235}U	^{236}U	^{238}U	Mass Assignment in mg of ^{235}U
S-2π-1	U-1	0.028	99.86	0.068	0.054	--
Ag-1	U-1	"	"	"	"	10.23 ± 0.20
S-4π-400	U-3	0.168	99.505	0.026	0.301	7.811 ± 0.039
Ag-10	U-2	0.047	99.564	0.311	0.078	13.91 ± 0.28
Ag-20	U-2	"	"	"	"	11.24 ± 0.22
S-2π-4	U-4	0.843	93.40	0.317	5.436	0.3856 ± 0.0019
S-2π-2	U-5	1.03	98.41	0.457	0.103	--
S-2π-5	U-6	0.027	98.37	0.056	1.54	--

TABLE III. Energy Ranges and Detectors Used in Shape Measurements.

Energy Range in keV	Fission Detector	Sample	Neutron Detector
400 - 2800	FT-IC	S-2π-2	BND
35 - 2800	2π-GSC	S-2π-1	GND - Water
500 - 3500	"	"	GND - $VOSO_4$ + Water
500 - 2800	"	"	GND - $MnSO_4$ + Water
160 - 1300	"	"	GND - Paraffin
35 - 110, 250	"	S-2π-5	Li-Glass

TABLE IV. Corrections and Uncertainties of the Final Result Caused by the Corrections for Shape Measurements with the BND.

Effect	Range of Corrections in per cent	Uncertainties Caused by the Corrections in per cent
Attenuation in Air	5 - 12	0.5 - 1.2
Attenuation in Chamber	1.5 - 2.5	0.2 - 0.3
Second Neutron Group	0 - 13	0.0 - 1.0
Inscatter from Fission Counter	1.4 - 2.5	0.3 - 0.5
Inscatter from Target	0.6 - 1.0	0.3 - 0.5
Inelastic Scattering in Fission Counter	0.0 - 0.2	0.1
Non- ^{235}U Isotopes	0.2 - 1.5	0.1 - 0.2
Angular Distribution of Source	1.0 - 2.5	0.2 - 0.5
Energy Dependence of Fission Counter Efficiency	0.1 - 0.5	0.1 - 0.2
BND Efficiency	3.4 - 11.5	1.0 - 2.0
Backscatter to BND	0.0 - 1.5	0.2 - 0.5
Collimator Transmission	0.5 - 1.5	0.2 - 0.3

TABLE V. Results for the Shape of the ^{235}U Fission Cross Section Measured with the BND

E_n in keV	$\pm\Delta E_n$ in keV	σ in mb	$\Delta\sigma$ in mb	E_n in keV	$\pm\Delta E_n$ in keV	σ in mb	$\Delta\sigma$ in mb
399	30	1223	44	1700	22	1260	33
						} 1255	
499	30	1164	21	1702	22	1249	32
600	28	1107	18				
685	27	1136	20	1750	22	1258	33
799	27	1134	21	1801	21	1266	33
						} 1249	
847	12	1115	22	1801	21	1232	32
867	12	1156	24				
887	12	1147	25	1850	21	1283	33
897	12	1157	27	1903	21	1282	33
917	12	1174	24	1951	21	1284	33
947	12	1220	27	2000	21	1285	33
966	12	1217	28	2012	20	1300	32
997	12	1194	30	2053	20	1285	33
1017	12	1190	33	2093	20	1268	32
						} 1265	
1047	12	1170	30	2093	20	1261	33
1100	25	1200	26				
1185	23	1205	29	2133	20	1272	33
1401	23	1196	30	2202	20	1290	32
						} 1288	
1491	23	1208	31	2203	20	1286	35
		} 1214					
1492	23	1219	30				
				2253	20	1259	34
1550	23	1225	32	2302	20	1281	34
1601	22	1233	32	2403	19	1315	32
		} 1236					
1601	22	1238	32	2703	18	1243	32
				2803	18	1233	31
1650	22	1261	33				

TABLE VI. Results for the Shape of the ^{235}U Fission Cross Section Using the GND (W = Water-, P = Paraffin-, Mn-Manganese-, V = Vanadium-Moderator).

E_n in keV		$\pm \Delta E_n$ in keV	σ in mb		$\Delta\sigma$ in mb	GND Moderator
35		3	2017		76	W
47		5	1824		60	W
68		5	1690		45	W
84		5	1579		38	W
97		8	1579		35	W
121		8	1502		31	W
141	143	15	1426	1409	21	P
144		23	1392		33	W
174	177	10	1379	1371	28	W
179		25	1362		18	P
194		23	1384		42	W
218		18	1348		46	W
231		25	1326		18	P
273		35	1358		40	W
282		25	1290		20	P
297		10	1259		29	W
393	396	25	1222	1192	21	P
399		35	1161		28	W
427	431	29	1214	1179	27	W
434		15	1144		35	W
502	508	31	1132	1133	21	W
509		16	1128		21	Mn
514		26	1139		24	V
556		28	1190		18	W
593	599	25	1154	1139	15	P
604		30	1125		18	W

TABLE VI.(Cont'd)

E_n in keV		$\pm \Delta E_n$ in keV	σ in mb		$\Delta\sigma$ in mb	GND Moderator
647		27	1113		17	W
692		25	1104		18	W
706	709	29	1108	1104	24	W
711		24	1099		24	Mn
757		24	1119		20	W
807	808	28	1078	1102	23	W
809		24	1126		25	Mn
861		23	1158		27	Mn
887		28	1175		26	W
897	900	25	1172	1143	18	P
903		27	1114		24	W
944		45	1252		22	W
957	959	27	1238	1228	28	W
960		23	1218		31	Mn
997		25	1212		24	P
1036	1039	51	1225	1210	26	W
1041		45	1195		26	Mn
1103	1106	44	1198	1197	23	W
1109		43	1195		27	V
1194	1197	25	1246	1232	24	P
1199		64	1217		26	W
1227		42	1239		27	Mn
1278		41	1205		21	W
1300		43	1154			V
1406	1410	41	1244	1243		V
1414		48	1241			W

TABLE VI. (Cont'd)

E_n in keV		$\pm \Delta E_n$ in keV	σ in mb		$\Delta\sigma$ in mb	GND Moderator
1421		40	1263		28	Mn
1498	1507	40	1225	1260	28	V
1515		40	1294		26	W
1605		55	1299		29	W
1704		74	1286		28	V
1818		73	1285		29	V
1819	1820	44	1302	1289	32	W
1823		35	1279		29	Mn
1911		33	1294		33	Mn
1970		72	1338		31	V
2007		70	1344		33	V
2010	2015	53	1397	1368	32	W
2027		28	1363		32	Mn
2107		68	1338		35	V
2204		67	1337		36	V
2304		66	1354		37	V
2499		64	1250		36	V
2802		61	1252		39	V
2820	2820	45	1315	1294	41	W
2837		30	1315		34	Mn
3000		58	1234		40	V
3500		53	1192		45	V

TABLE VII. Results from Shape Measurements Relative to $^{6}Li(n,\alpha)T$.

E_n in keV	$\pm \Delta E_n$ in keV	$\sigma_{n,\alpha}$ in mb	σ_f in mb	$\pm\Delta\sigma_f$ in mb
34.5	5	820	1996	60
42	5	750	1856	54
45.5	5	725	1866	54
60	5	665	1795	52
75	5	635	1737	51
83	5	630	1629	47
90	5	625	1579	44
101	5	625	1589	44
109	5	630	1574	44
250	4	3000	1320	norm.

TABLE VIII. Summary of Absolute Measurements.

E_n in keV	Fission Detector	Foil	Neutron Flux Determination
800	FT-IC	S-2π-4	Small BND
3500	4π-GSC	S-4π-400	Large BND
500	"	"	Cf-Source Calibrated Vanadium Bath
448	SS-IC-1	AG-1	Associated Activity
530	"	"	"
574	"	"	"
638	"	"	"
650	"	"	"
552	SS-IC-2	AG-10	"
554	"	"	"
602	"	"	"
600	SS-IC-3	AG-20	"

TABLE IX. Corrections, Uncertainties Caused by the Corrections, and other Uncertainties for Absolute Measurements.

Effect	Correction and Uncertainty in Per Cent Small Detector (800 keV)		Large Detector (3500 keV)	
Attenuation in Air	7.9	0.8	3.0	0.3
Second Neutron Group	1.7	0.2	0.8	0.1
Attenuation in Fission Chamber	2.0	0.2	0.7	0.1
Inscatter from Fission Chamber	0.8	0.4	0.5	0.1
Fission in Non-^{235}U Isotopes	0.9	0.1	0.3	0.1
BND-Efficiency	4.0	1.0	3.3	1.0
Angular Distribution of Source Reaction	0.5	0.1		
Neutron Return to BND	0.5	0.3		
BND-Entrance Window	0.3	0.1		
Collimator Transmission	0.8	0.2	0.5	0.2
Inscatter from Ta-Cup	0.7	0.3		
Inelastic Scattering in Backing	0.1	0.1		
Energy Dependence of ϵ_f	0.2	0.1	0.3	0.1
Fission Counting Efficiency (ϵ_f)	1.9	0.5	5.1	1.0
Total Contribution from Uncertainties of Corrections		1.6		1.5
Uncertainty of Mass Assignment		0.5		0.5
Statistical Uncertainty of Count Rates		1.2		1.4
Uncertainty of Background Subtraction and Integration of Count Rates		0.5		0.5
Uncertainty of Geometrical Factors		1.2		0.5
Total Uncertainty of Result		2.4		2.2

TABLE X. Corrections for Scattered Neutrons.

Effect from Scattering	Correction in per cent
Inner Sphere	2.5 - 4.2
Outer Sphere	0.3 - 0.6
Teflon Roads	0.4
Teflon Rings	0.7
Air Cooling Tube	0.1
Target Construction	0.5
Inelastic Scattering	0.4
Total Correction	4.9 - 6.9

TABLE XI. Results for the Fission Cross Section from the Associated Activity Technique

E_n in keV		$\pm \Delta E_n$ in keV	Detector	σ in mb		$\pm\Delta\sigma$ in mb
448		60	Ag 1	1220		44
552	553	60	Ag 1	1121*	1116	43
553		50	Ag 10	1110		41
600	601	59	Ag 20	1116	1108	41
602		52	Ag 10	1100		40
644		65	Ag 1	1101*		42

*Values previously reported (26) were based on the destructive (colometric) analysis of the ^{235}U amount on the spheres only.

TABLE XII. Final Results for the Fission Cross Section of ^{235}U

(Uncertainty ± 3 per cent)

E_n in keV	σ in mb	E_n in keV	σ in mb
35	2006	800	1110
40	1931	840	1120
45	1856	860	1135
50	1818	890	1161
55	1794	920	1185
60	1772	950	1214
70	1710	980	1209
80	1647	1000	1207
90	1588	1200	1204
100	1555	1400	1213
120	1493	1500	1226
140	1437	1800	1279
170	1387	1900	1290
200	1357	2000	1294
250	1307	2100	1292
300	1268	2200	1285
350	1228	2400	1266
400	1201	2600	1253
500	1160	3000	1224
600	1125	3500	1192
700	1110		

Figure Captions

Fig. 1 2π Gas Scintillation Counter and Fission Fragment Pulse Height Spectra Obtained with a 400 $\mu g/cm^2$ Uranium Foil.

Fig. 2 4π Gas Scintillation Counter and Fission Fragment Pulse Height Sum Spectra Obtained with a 60 $\mu g/cm^2$ Uranium Foil.

Fig. 3 Spherical Fission Counter and Fission Fragment Pulse Height Spectra Obtained with a 60 $\mu g/cm^2$ Uranium Deposit.

Fig. 4 Fast-Timing Ionization Chamber and Fission Fragment Pulse Height Spectra Obtained with a 100 $\mu g/cm^2$ Uranium Foil.

Fig. 5 Specific ^{235}U Mass of Material U-3 Obtained by Different Techniques.

Fig. 6 Efficiency of the Small Black Neutron Detector.

Fig. 7 Time-of-Flight and Neutron Pulse Height Spectra Obtained with the Black Neutron Detector.

Fig. 8 Efficiencies of the Grey Neutron Detector with a Vanadium Sulfate Solution-Moderator for Different γ-Spectrum Ranges.

Fig. 9 Schematic Experimental Setup for Shape Measurements with the Black Neutron Detector and the Grey Neutron Detector.

Fig.10 Results of Shape Measurements with the Black Neutron Detector.

Fig.11 Total Correction Applied for the Shape Measurements with the Grey Neutron Detector.

Fig.12 Results of Shape Measurements Obtained with the Grey Neutron Detector and Li-Glass Detector.

Fig.13 Schematic Experimental Setup for Absolute Measurements with the Large Black Neutron Detector and the Vanadium Bath.

Fig.14 Calibration Factors for the ^{51}Cr Activity Measurement with the NaI(Tl)-Detector.

Fig.15 Absolute Values Obtained in the Present Experiments and the Final Result.

Fig.16 Comparison of Present Results with Other Data for the ^{235}U Fission Cross Section.

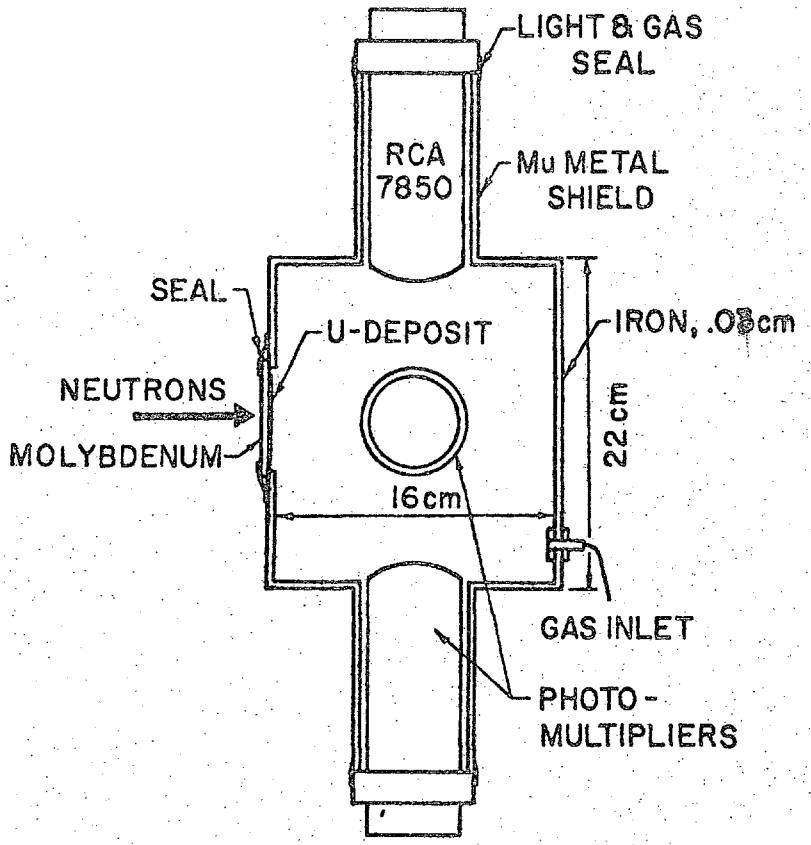
LIGHT & GAS SEAL
RCA 7850
Mu METAL SHIELD
SEAL
U-DEPOSIT
IRON, .08cm
NEUTRONS
MOLYBDENUM
22cm
16cm
GAS INLET
PHOTO-MULTIPLIERS

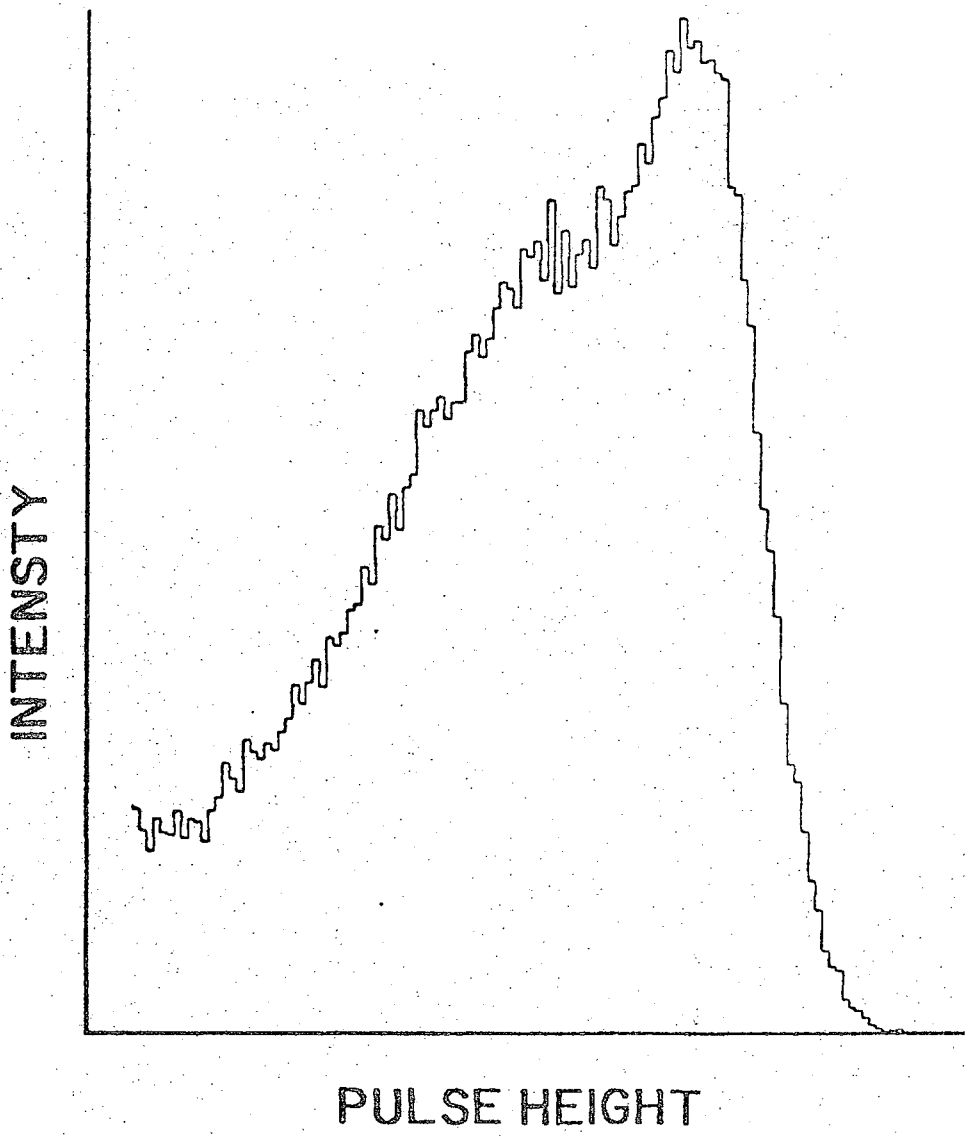
INTENSTY
PULSE HEIGHT

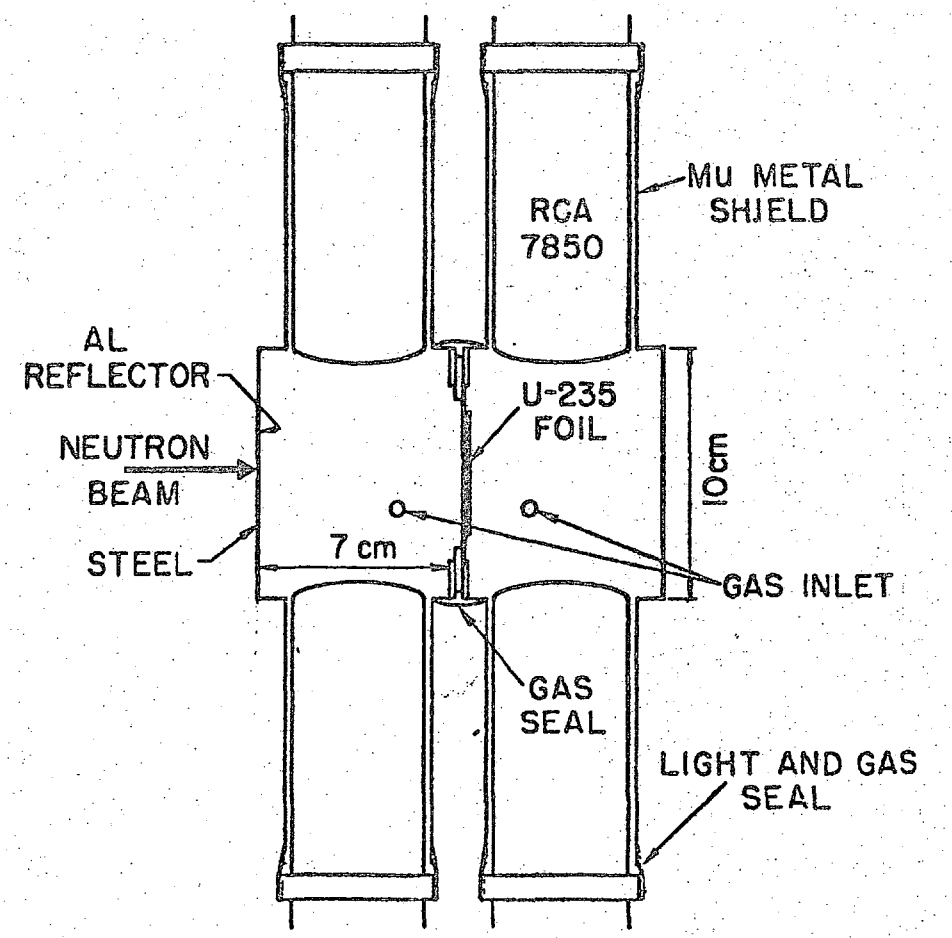
RCA
7850
Mu METAL
SHIELD
AL
REFLECTOR
NEUTRON
BEAM
STEEL
U-235
FOIL
10cm
7 cm
GAS INLET
GAS
SEAL
LIGHT AND GAS
SEAL

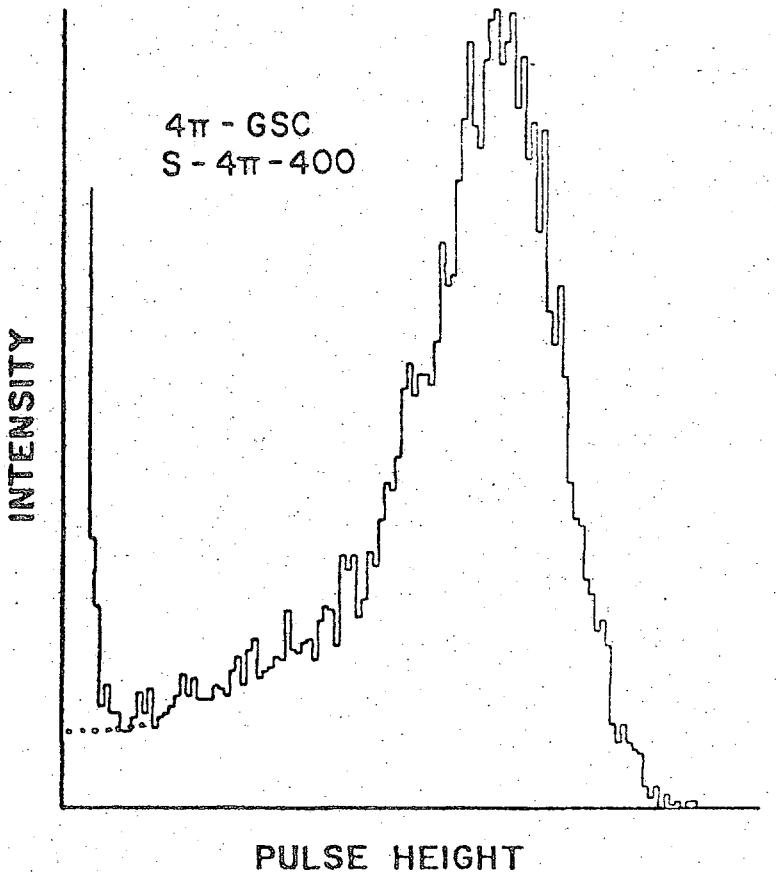
4π - GSC
S - 4π - 400
INTENSITY
PULSE HEIGHT

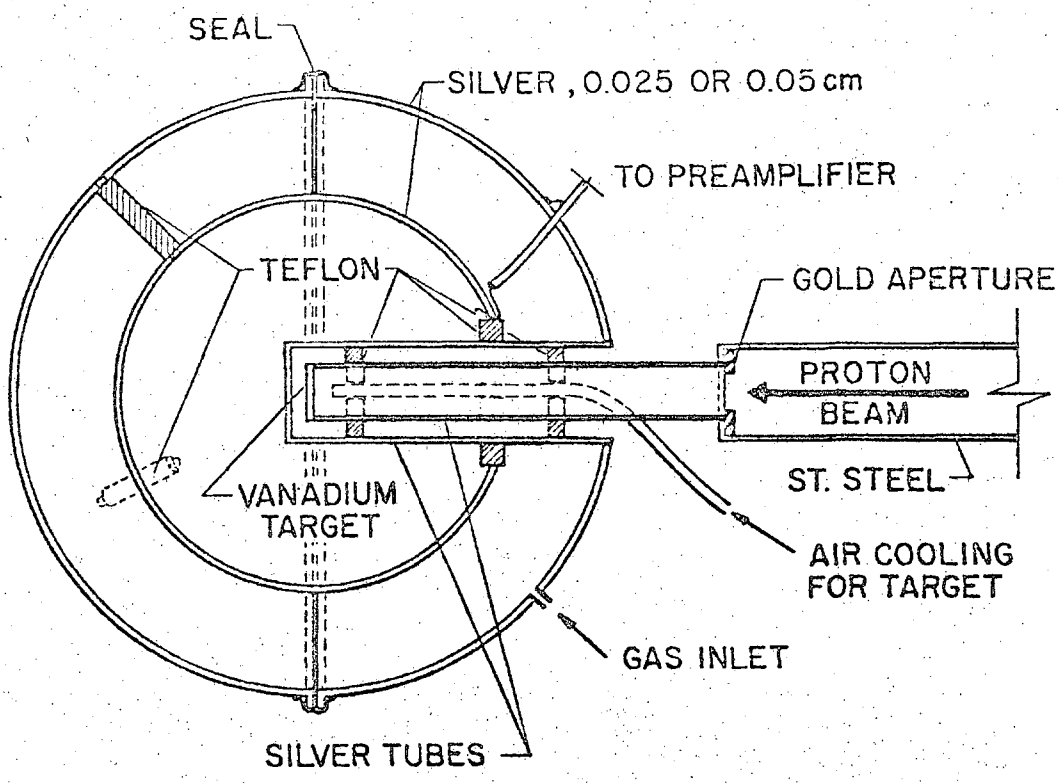
SEAL
SILVER , 0.025 OR 0.05 cm
TO PREAMPLIFIER
TEFLON
GOLD APERTURE
PROTON
BEAM
ST. STEEL
VANADIUM
TARGET
AIR COOLING
FOR TARGET
GAS INLET
SILVER TUBES

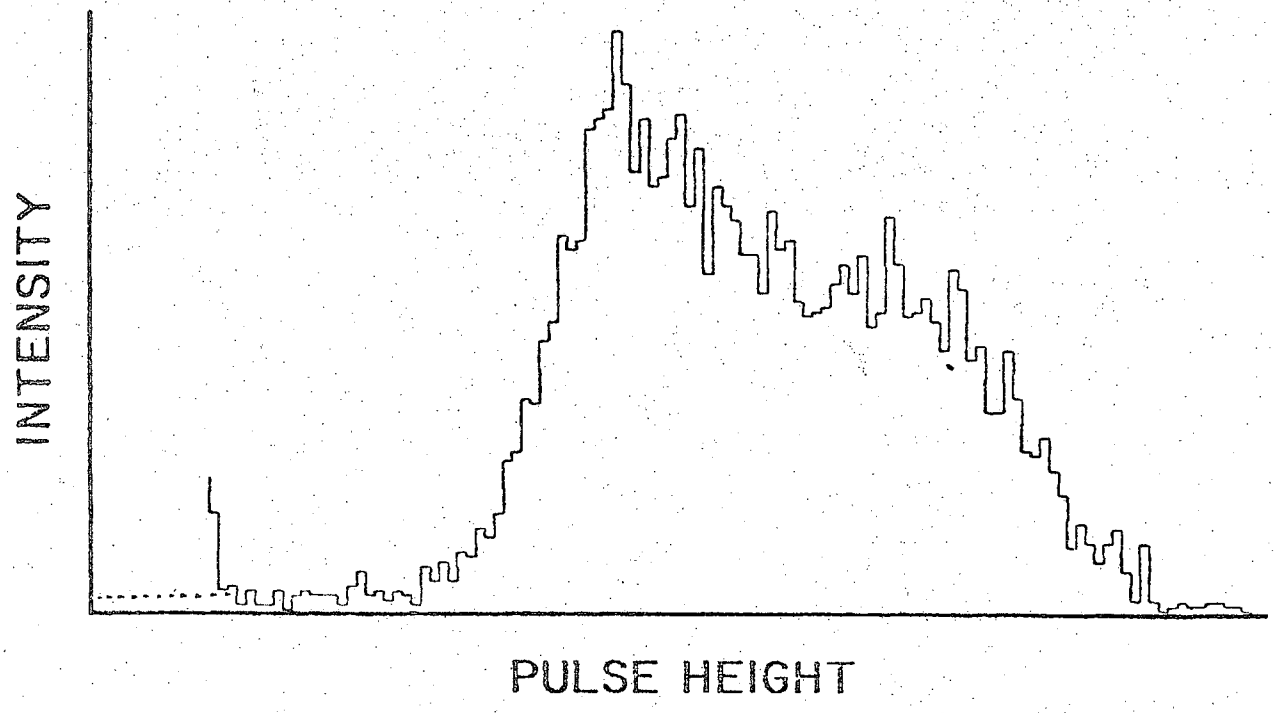
INTENSITY
PULSE HEIGHT

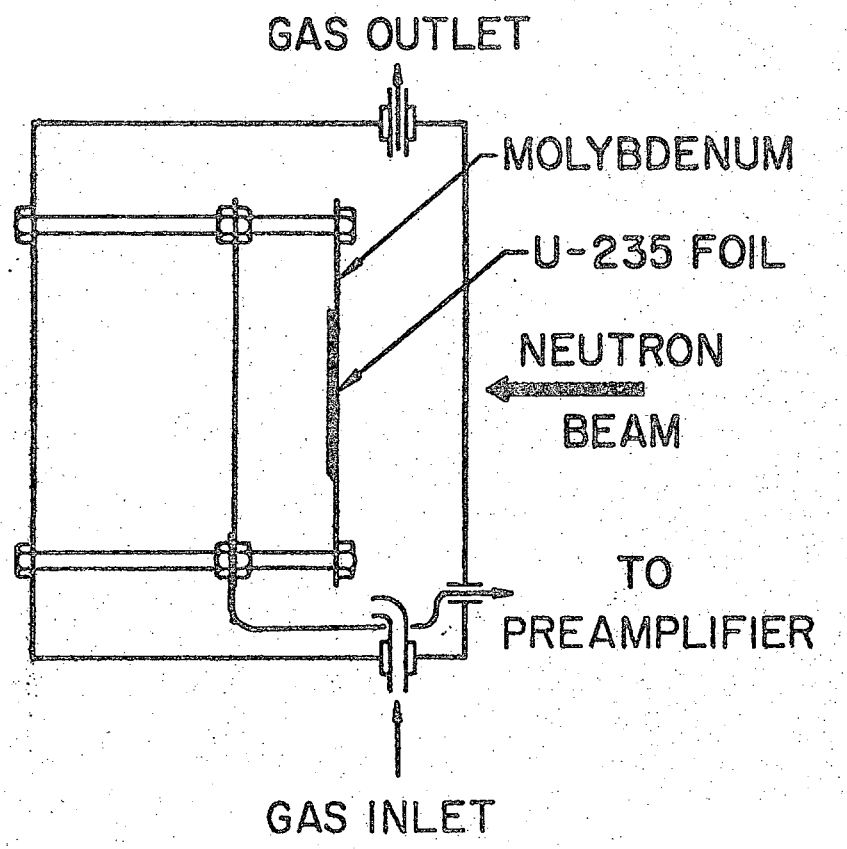
GAS OUTLET
MOLYBDENUM
U-235 FOIL
NEUTRON
BEAM
TO
PREAMPLIFIER
GAS INLET

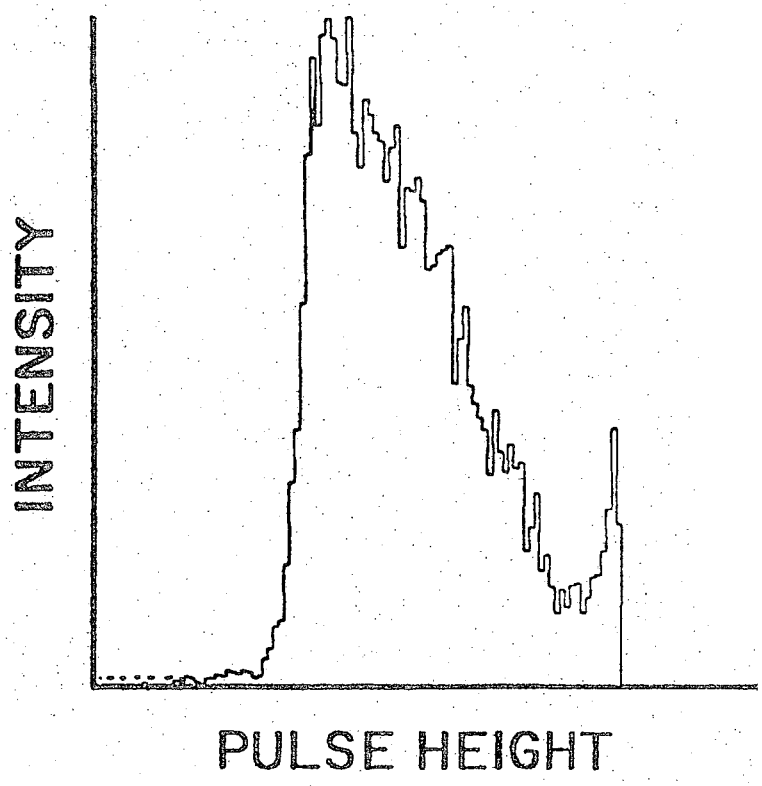
INTENSITY
PULSE HEIGHT

Specific Mass, Hg/αps
2.20
2.15
2.10
2.05
EURATOM
ANL-ARGONNE
ANL-IDAHO
ANL-ARGONNE
ANL-ARGONNE
ANL-IDAHO
ANL-ARGONNE
Obtained from
Isotopic Composition & Half-Lives
Colorimetric Analysis & α-Counting
Isotopic Dilution & α-Counting
Average Values

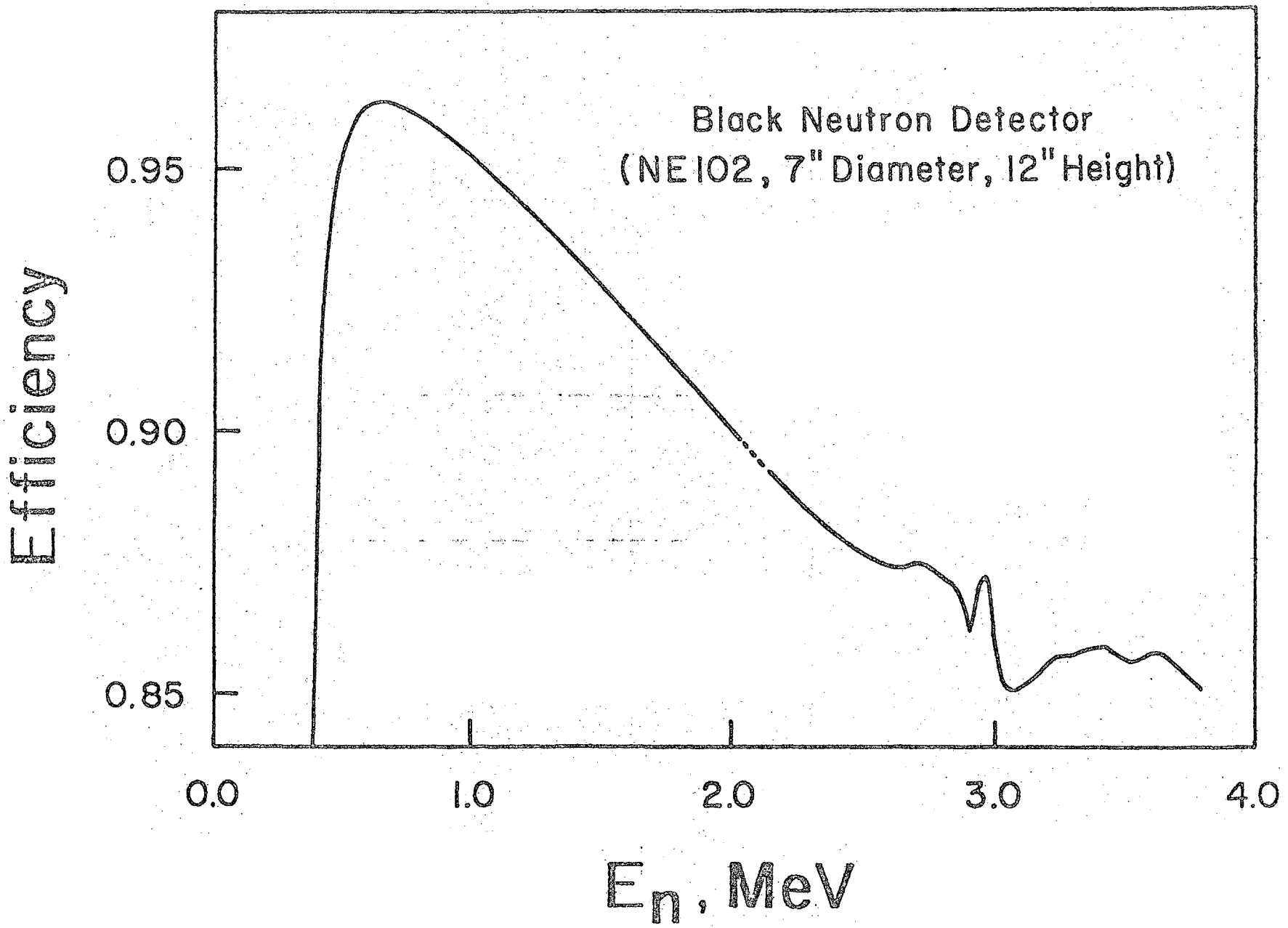
Black Neutron Detector
(NE102, 7" Diameter, 12" Height)
Efficiency
0.95
0.90
0.85
0.0
1.0
2.0
3.0
4.0
E_n, MeV

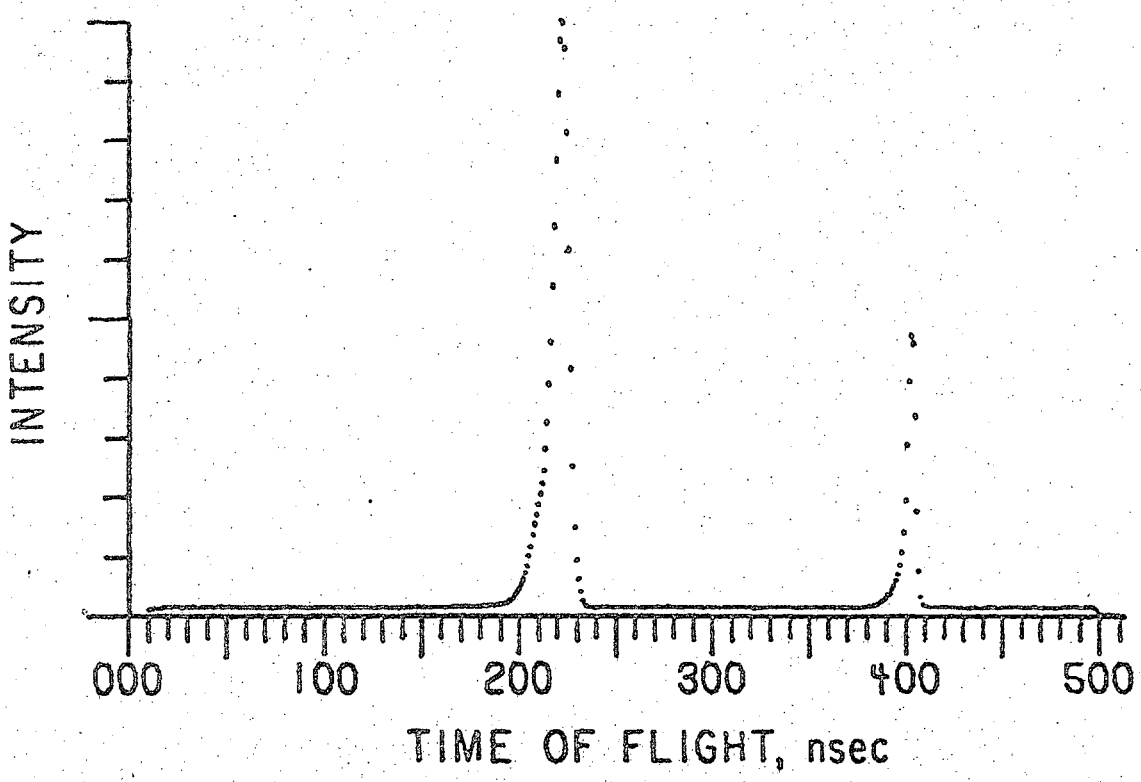
INTENSITY
000
100
200
300
400
500
TIME OF FLIGHT, nsec

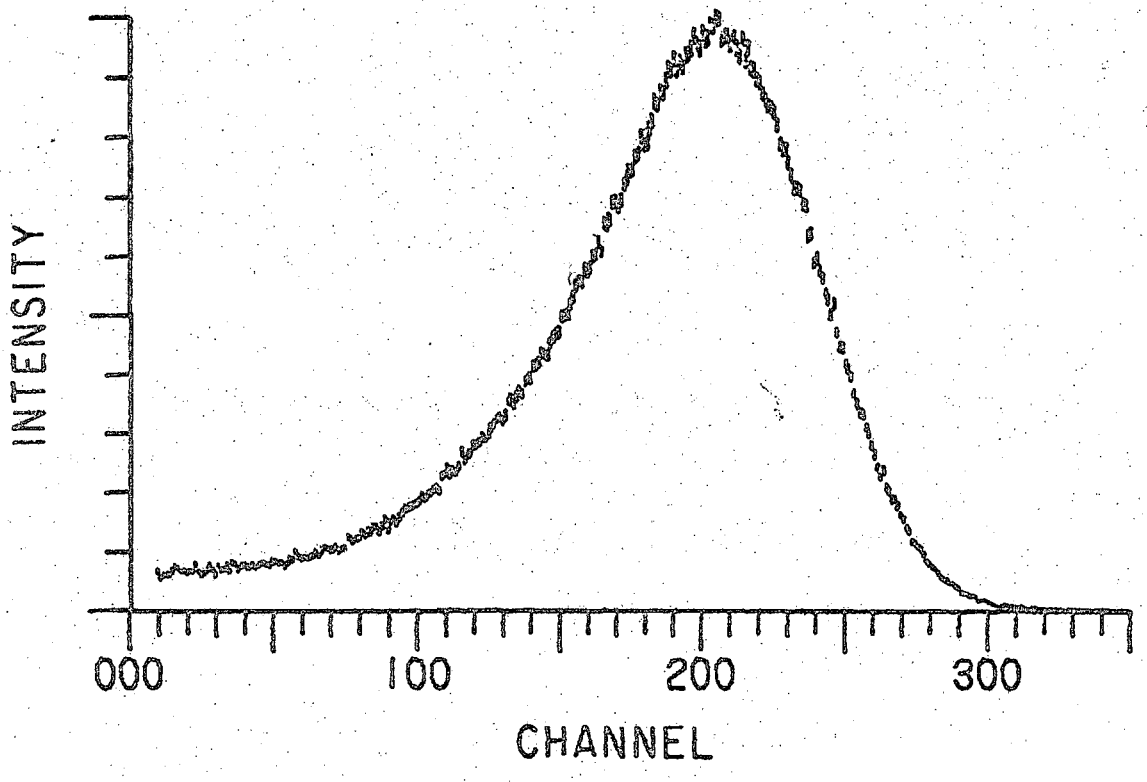
INTENSITY
000
100
200
300
CHANNEL

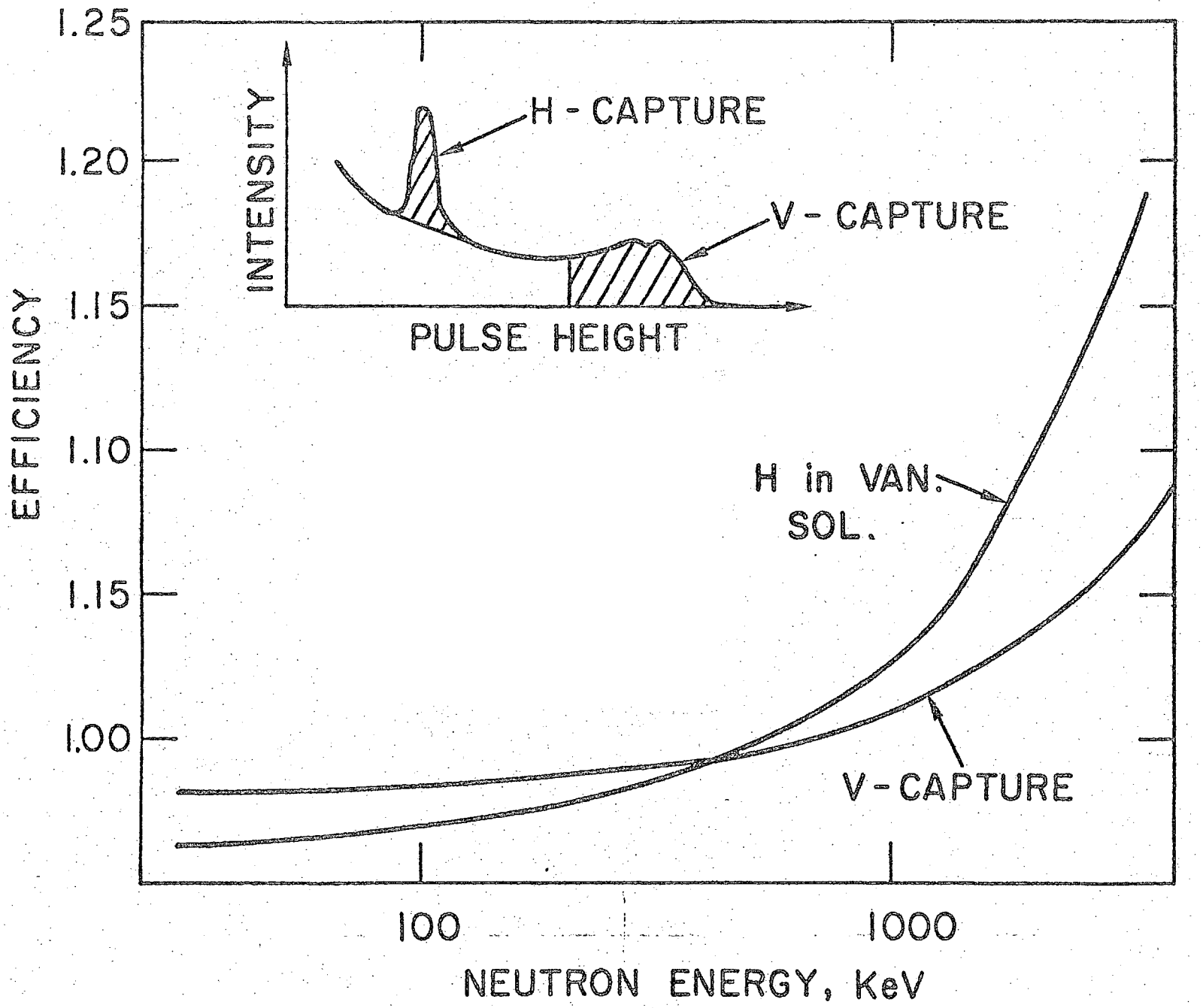
1.25
1.20
1.15
1.10
1.15
1.00
EFFICIENCY
INTENSITY
H - CAPTURE
V - CAPTURE
PULSE HEIGHT
H in VAN.
SOL.
V - CAPTURE
100
1000
NEUTRON ENERGY, KeV

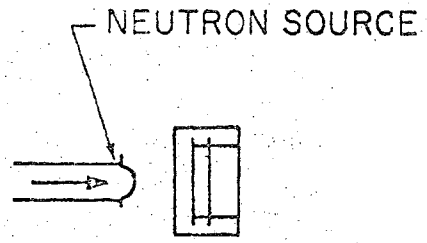

FISSION DETECTOR

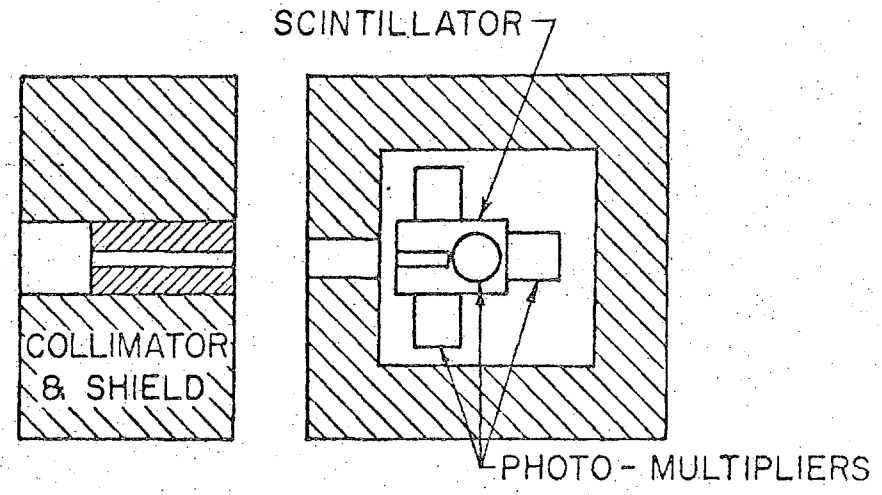

BLACK NEUTRON DETECTOR
& SHIELDING

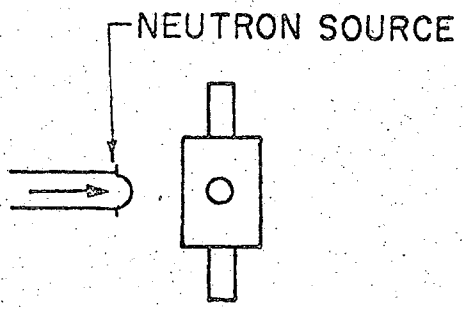

FISSION COUNTER

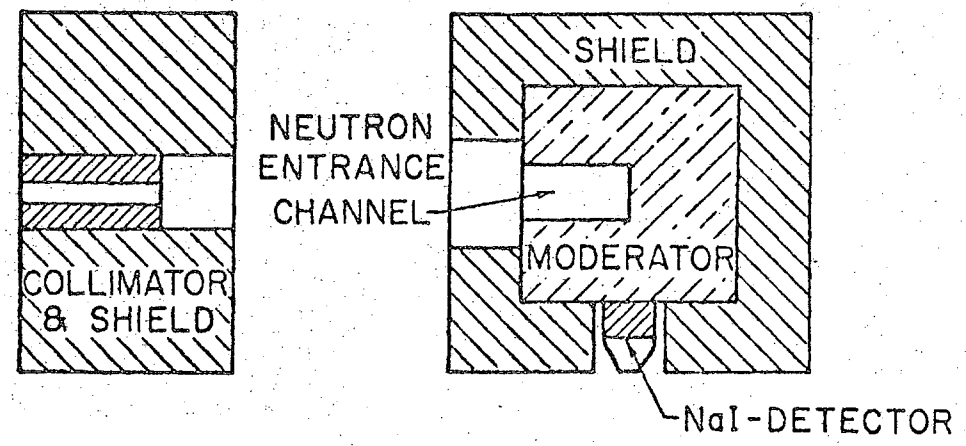

GREY NEUTRON DETECTOR

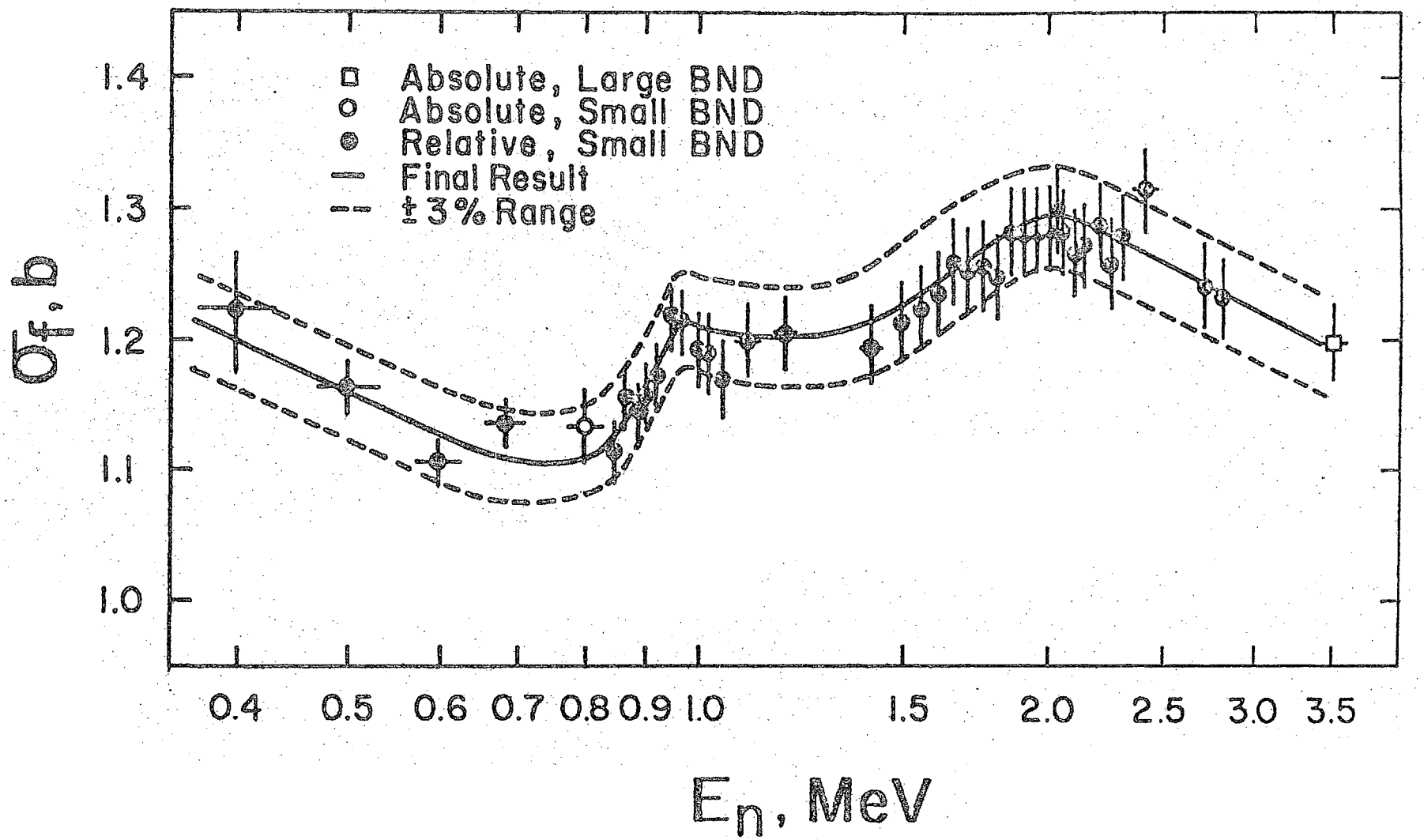
Absolute, Large BND
Absolute, Small BND
Relative, Small BND
Final Result
± 3% Range
1.4
1.3
1.2
1.1
1.0
0.4
0.5
0.6
0.7
0.8
0.9
1.0
1.5
2.0
2.5
3.0
3.5
En, MeV

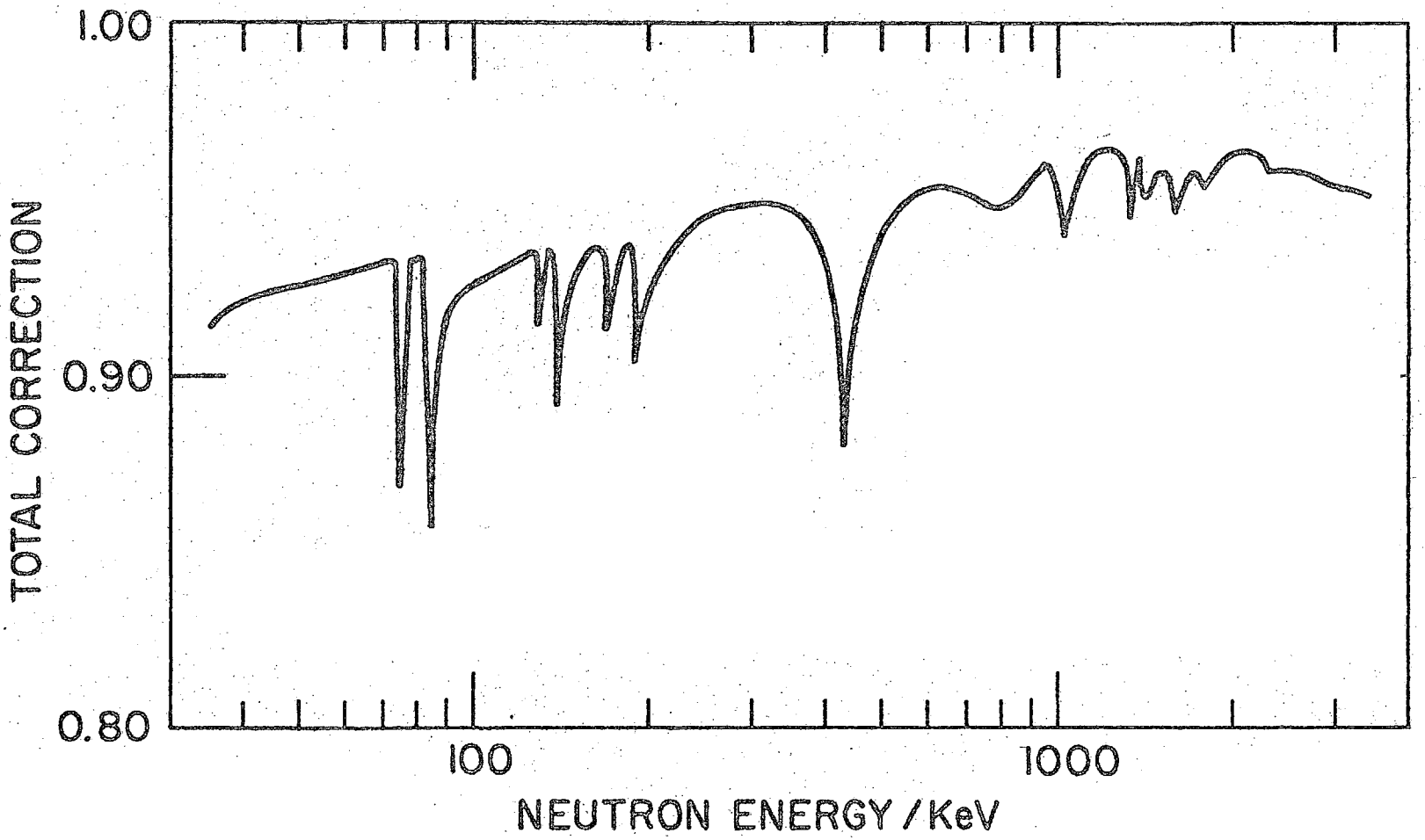
1.00
0.90
0.80
TOTAL CORRECTION
100
1000
NEUTRON ENERGY / KeV

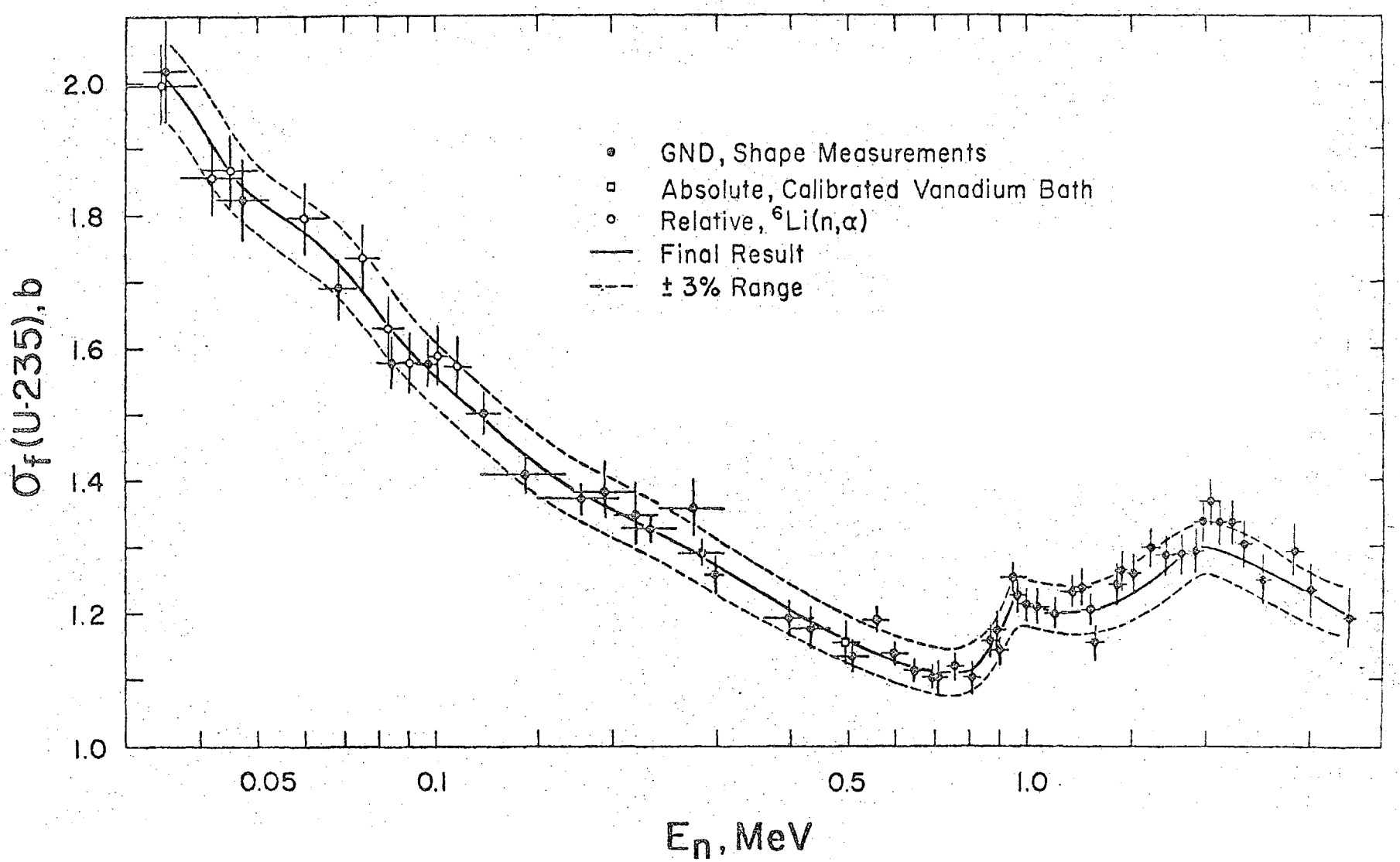
GND, Shape Measurements
Absolute, Calibrated Vanadium Bath
Relative, $^{6}Li(n,\alpha)$
Final Result
± 3% Range
σ_f(U-235), b
2.0
1.8
1.6
1.4
1.2
1.0
0.05
0.1
0.5
1.0
E_n, MeV

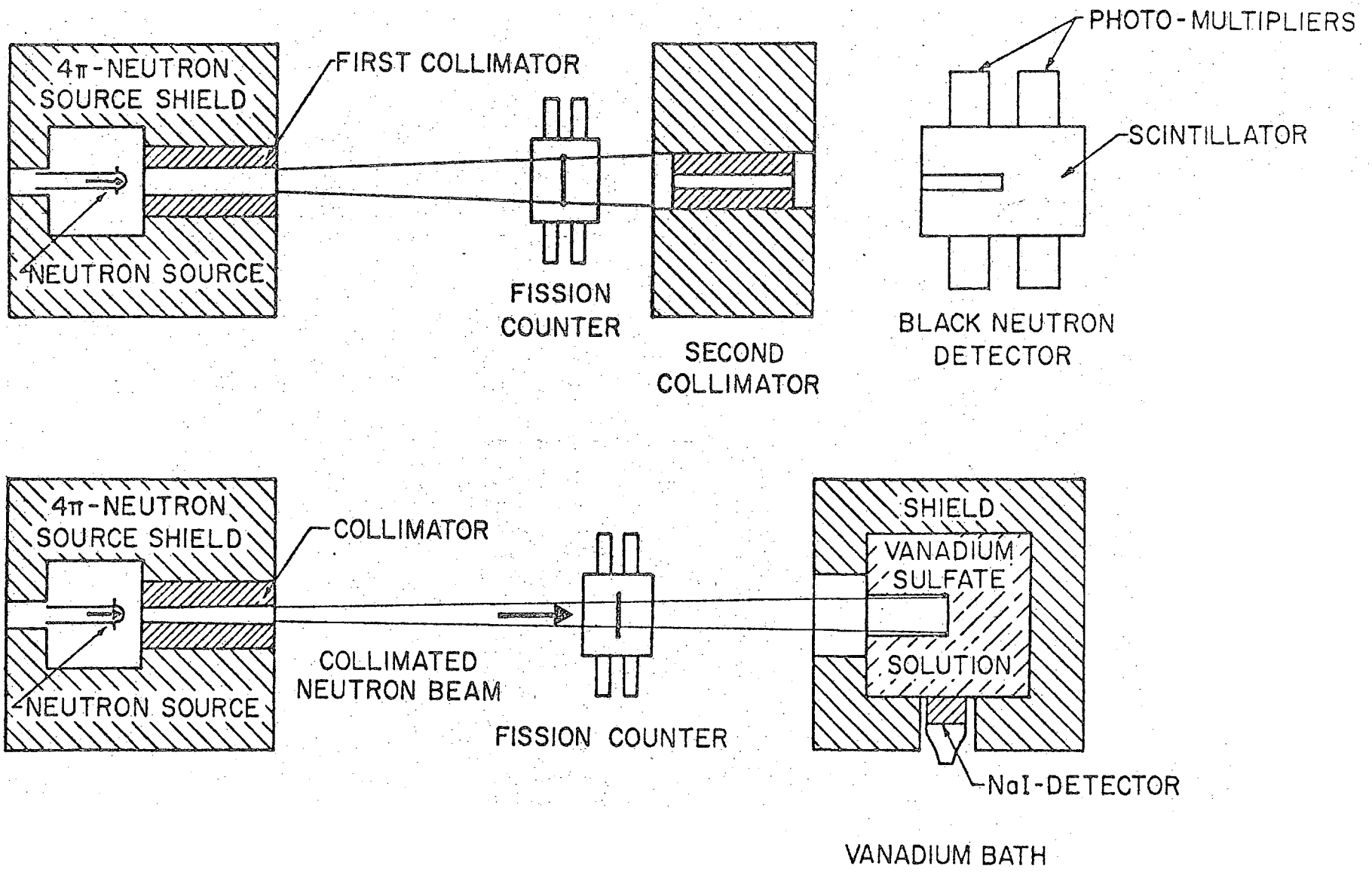
4π-NEUTRON SOURCE SHIELD
FIRST COLLIMATOR
NEUTRON SOURCE
FISSION COUNTER
SECOND COLLIMATOR
PHOTO-MULTIPLIERS
SCINTILLATOR
BLACK NEUTRON DETECTOR
4π-NEUTRON SOURCE SHIELD
COLLIMATOR
NEUTRON SOURCE
COLLIMATED NEUTRON BEAM
FISSION COUNTER
SHIELD
VANADIUM SULFATE
SOLUTION
NaI-DETECTOR
VANADIUM BATH

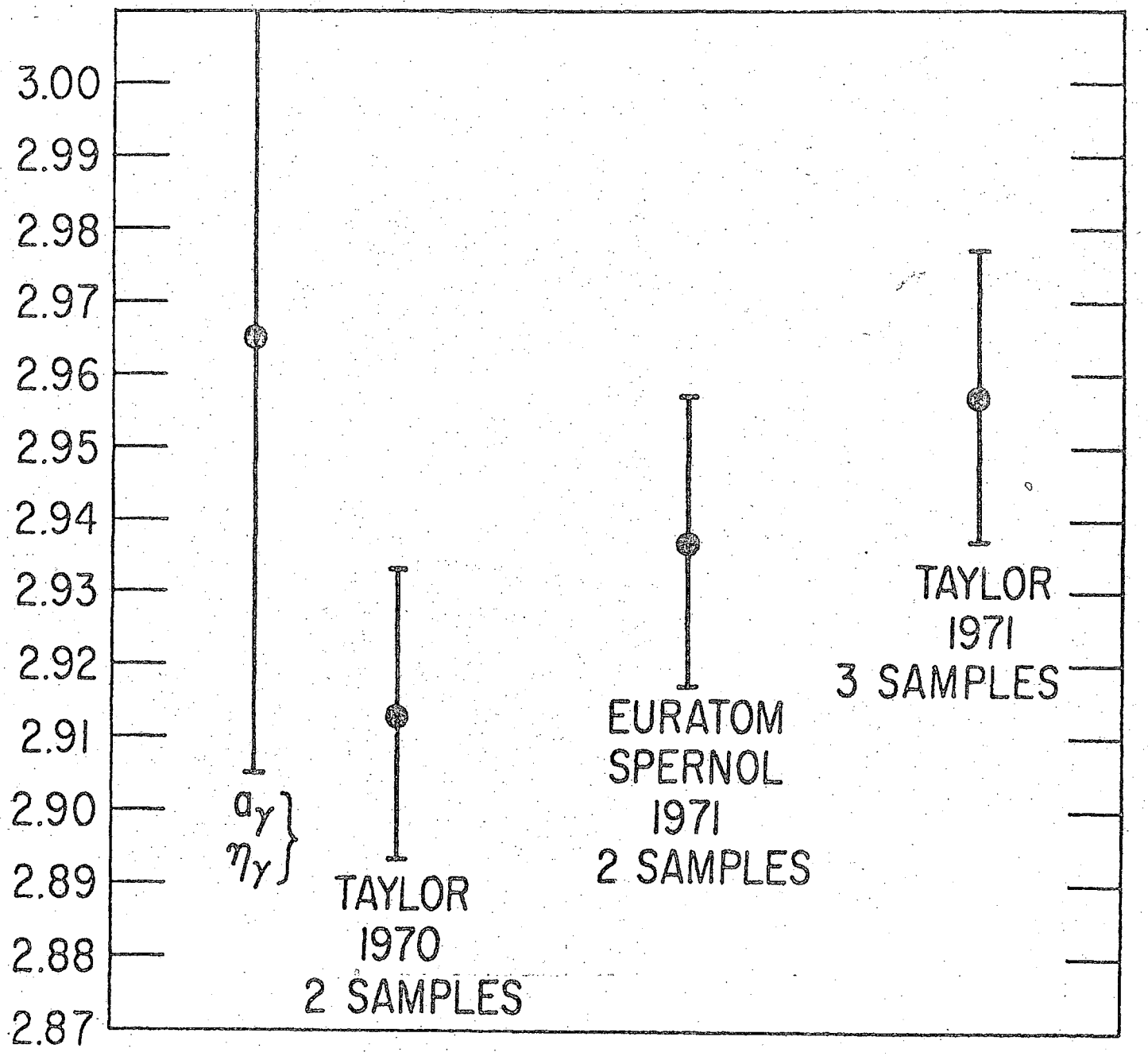
3.00
2.99
2.98
2.97
2.96
2.95
2.94
2.93
2.92
2.91
2.90
2.89
2.88
2.87
a_γ
η_γ
TAYLOR
1970
2 SAMPLES
EURATOM
SPERNOL
1971
2 SAMPLES
TAYLOR
1971
3 SAMPLES

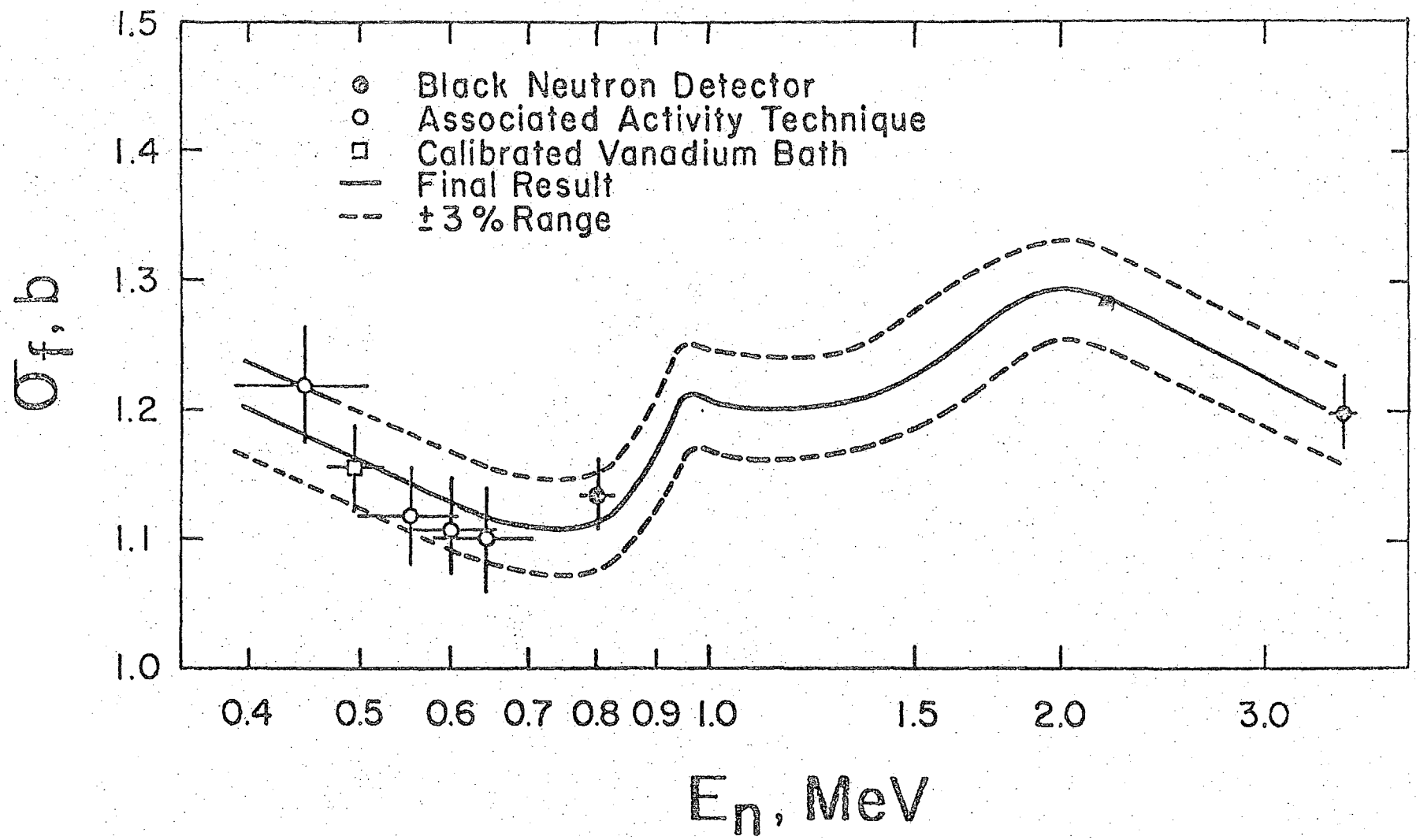
Black Neutron Detector
Associated Activity Technique
Calibrated Vanadium Bath
Final Result
± 3 % Range
σf, b
1.5
1.4
1.3
1.2
1.1
1.0
0.4
0.5
0.6
0.7
0.8
0.9
1.0
1.5
2.0
3.0
En, MeV

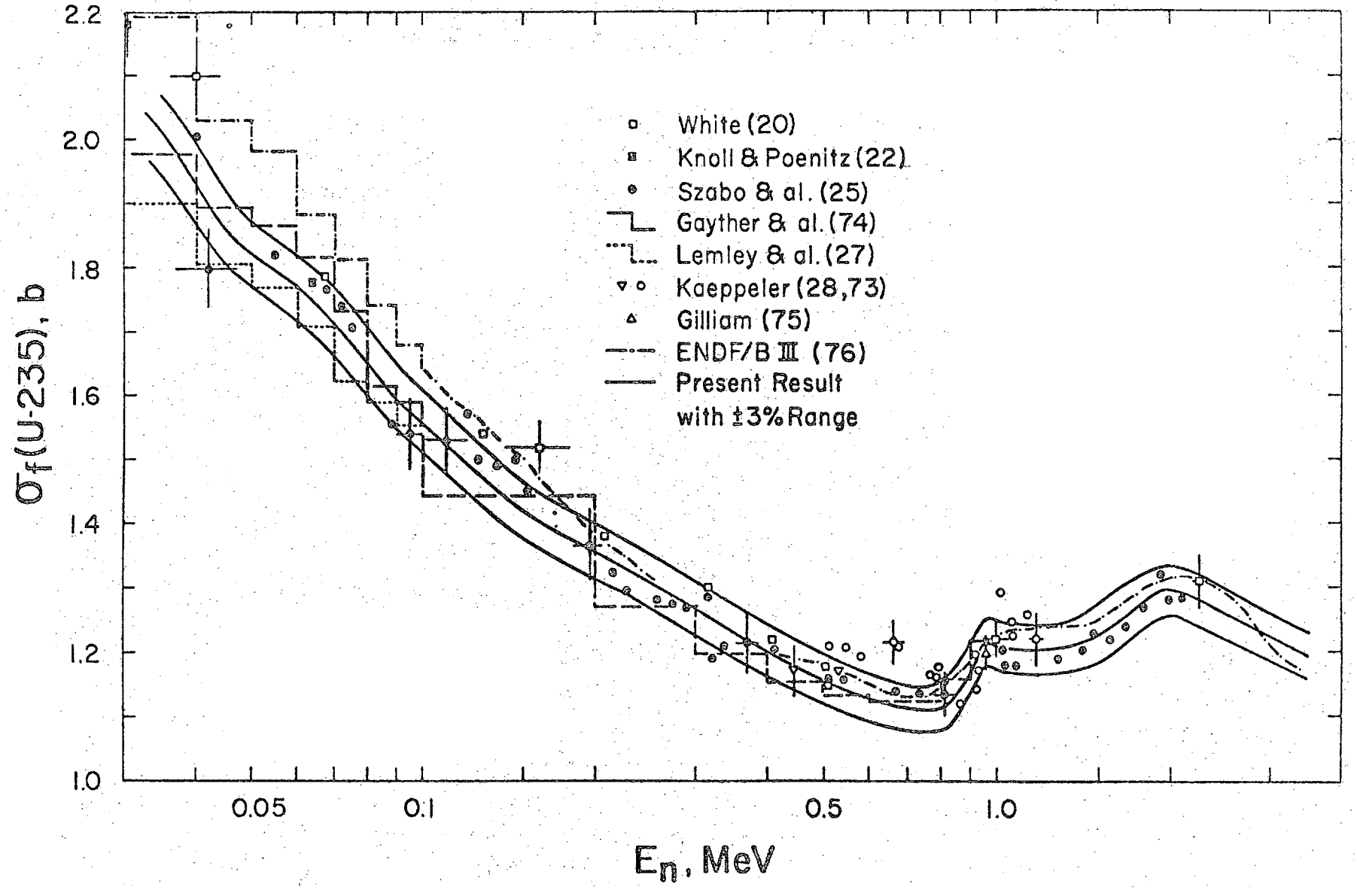
2.2
2.0
1.8
1.6
1.4
1.2
1.0
0.05
0.1
0.5
1.0
σ_f(U-235), b
E_n, MeV
White (20)
Knoll & Poenitz (22)
Szabo & al. (25)
Gayther & al. (74)
Lemley & al. (27)
Kaeppeler (28,73)
Gilliam (75)
ENDF/B III (76)
Present Result
with ±3% Range